Ph.D. DISSERTATION

Synchronization and Group Formation for Infrastructure-less Public Safety Networks

인프라가 없는 환경에서의 재난 통신망을 위한 동기화 및 그룹 형성 기법

BY

SEONIK SEONG

AUGUST 2016

DEPARTMENT OF ELECTRICAL ENGINEERING AND
COMPUTER SCIENCE
COLLEGE OF ENGINEERING
SEOUL NATIONAL UNIVERSITY

Ph.D. DISSERTATION

Synchronization and Group Formation for Infrastructure-less Public Safety Networks

인프라가 없는 환경에서의 재난 통신망을 위한 동기화 및 그룹 형성 기법

BY

SEONIK SEONG

AUGUST 2016

DEPARTMENT OF ELECTRICAL ENGINEERING AND
COMPUTER SCIENCE
COLLEGE OF ENGINEERING
SEOUL NATIONAL UNIVERSITY

Synchronization and Group Formation for Infrastructure-less Public Safety Networks

인프라가 없는 환경에서의 재난 통신망을 위한 동기화 및 그룹 형성 기법

지도교수 이 광 복

이 논문을 공학박사 학위논문으로 제출함

2016년 8월

서울대학교 대학원

전기 컴퓨터 공학부

성 선 익

성선익의 공학박사 학위 논문을 인준함

2016년 8월

위 원 장: _____
부위원장: _____
위 원: _____
위 원: _____
위 원: _____

Abstract

A public safety network (PSN) has been developed as a special class of wireless communication network that aims to save lives and prevent property damage. PSNs have evolved separately from commercial wireless networks satisfying various requirements and regulatory issues associated with them. With growing needs for the transmission of multimedia data, existing voice-centric PSN technologies are facing hurdles in fulllfilling the demand for high capacity and different types of services. Mission-critical requirements for PSNs include the guaranteed dissemination of emergency information such as alarm texts, images, and videos of disasters even in the absence (or destruction) of cellular infrastructure. Many research projects have been launched to meet the mission-critical requirement of PSN, e.g., Aerial Base Station with Opportunistic Links for Unexpected & TEmporary events (ABSOLUTE), Alert for All (Alert4All), Mobile Alert InformAtion system using satellites (MAIA), and so on. The research projects include the emergency communications using satellite communications, aerial eNodeBs, and terrestrial radio access technologies. The approaches take advantages of inherent broadcasting and resilience with respect to Earth damages for disseminations of alert messages. In this dissertation, we limit our interests to terrestrial radio access technologies, e.g., LTE, TETRA, TETRAPOL, and DMR, because PSNs should be operational even in the low-class user equipments (UEs) that are lack of satellite communication functionalities.

In Chapter 2 of this dissertation, we propose a distributed synchronization algorithm for infrastructure-less public safety networks. The proposed algorithm aims to minimize the number of out-of-sync user equipments by efficiently forming synchronization groups and selecting synchronization reference UEs in a distributed manner. For the purpose, we introduce a novel affinity propagation technique which enables an autonomous decision at each UE based on local message-passing among neighboring

UEs. Our simulation results show that the proposed algorithm reduces the number of out-of-sync UEs by up to 40% compared to the conventional scan-and-select strategy. In Chapter 3 of this dissertation, we study an infrastructure-less public safety network where energy efficiency and reliability are critical requirements in the absence of cellular infrastructure, i.e., base stations and wired backbone lines. We formulate the IPSN group formation as a clustering problem. A subset of user equipments, called group owners (GOs), are chosen to serve as virtual base stations, and each non-GO UE, referred to as group member, is associated with a GO as its member. We propose a novel clustering algorithm in the framework of affinity propagation, which is a state-of-the-art message-passing technique with a graphical model approach developed in the machine learning field. Unlike conventional clustering approaches, the proposed clustering algorithm minimizes the total energy consumption while guaranteeing link reliability by adjusting the number of GOs. Simulation results verify that the IPSN optimized by the proposed clustering algorithm reduces the total energy consumption of the network by up to 31% compared to the conventional clustering approaches.

keywords: Infrastructure-less, public safety network, synchronization, group formation, affinity propagation

student number: 2008-22936

Contents

List of Tables

List of Figures

Chapter 1

INTRODUCTION

Recently, public safety networks (PSNs) have been studied extensively as a special communication system for emergency situations. Given their world-wide commercial success, the 3rd Generation Partnership Project Long-Term Evolution (3GPP-LTE) systems have become very attractive as a unified platform for PSNs [1, 2]. LTE-based PSNs can provide high-speed data transmissions that enable various types of multimedia services. LTE-based PSNs inherit other benefits in terms of transmission reliability and power efficiency based on advanced wireless techniques such as hybrid ARQ and interference mitigation. Furthermore, using pre-existing eco-systems can significantly reduce implementation costs. Many pioneering countries including the United States [3, 4] and South Korea [5] have established plans to evolve toward LTE-based PSNs. To cope with infrastructure-less environments such as the failure or destruction of network infrastructure, LTE-based PSNs enable direct communications between mobile devices to guarantee reliable communications in emergency situations [6, 7].

1.1 Distributed Synchronization Algorithm for Infrastructure-less Public Safety Networks

Unlike typical PSNs with infrastructure in which eNodeBs are responsible for synchronization by periodically broadcasting synchronization signals, infrastructure-less PSNs (IPSNs) face a challenge in that at least one user equipment (UE) should take over this responsibility. Thus, as a part of the current wireless standard activities, 3GPP task groups make great efforts to define UE-based synchronization procedures [8]. However, the issues of determining the synchronization reference (SyncRef) UEs that broadcast synchronization signals and the corresponding synchronization groups (SyncGroups) remain unsolved. Inappropriate choices of SyncRef UEs may lead to unnecessary power consumption of SyncRef UEs or to unacceptably low strength of the received signal at non-SyncRef UEs. In the worst case, non-SyncRef UEs that are located at the edge of a SyncGroup can experience a radio link failure (RLF), meaning the complete loss of the physical layer connection. Thus, SyncRef UEs and SyncGroups should be carefully determined considering the UE distribution.

The scan-and-select strategy is known to be a simple but efficient solution for the distributed synchronization of IPSNs, and hence, considered suitable for practical implementations [6]. The main idea is that a UE becomes a SyncRef UE if the UE cannot detect any synchronization signals or a UE becomes a member of the SyncGroup of the nearest SyncRef. Essentially, the scan-and-select strategy is a non-cooperative strategy because UEs do not share information or cooperate with others at the decision stage. This enables an autonomous decision at each UE based on independently collected local information. However, the scan-and-select strategy relies on greedy decisions, which make it clearly suboptimal.

In this dissertation, we propose a distributed algorithm that determines the SyncRef UEs and SyncGroups by introducing an affinity propagation (AP) framework [9]. AP is a novel clustering technique based on message-passing, and has been proven to be

a very efficient tool for various types of optimization problems in communication networks [10, 11, 12, 13]. By allowing local message-passing among neighboring UEs, the proposed algorithm efficiently solves the complicated optimization problem to determine SyncRef UEs, and enables an autonomous decision at each UE. This local cooperation based on message-passing allows the proposed algorithm to outperform the scan-and-select strategy significantly.

Our main contributions are summarized as follows:

- **SyncGroup organization:** We formulate the SyncRef selection problem in IPSN. Unlike the conventional synchronization algorithm, our formulation selects SyncRef UEs that minimize the expected number of out-of-sync UEs. The optimization problem is a complex integer programming.

- **Distributed and collaborative algorithm:** We propose a distributed and collaborative synchronization algorithm in the AP framework. The proposed algorithm iteratively exchanges and updates messages between neighboring UEs. In addition, we present how UEs initially participate in SyncRef selection procedures at the same timing without a central coordinator.

- **Reliable synchronization:** Our simulation results verify that the proposed algorithm reduces the average number of out-of-sync UEs in the network by up to 40% compared to the conventional synchronization algorithms. The robustness of the proposed algorithm to mobility and quantization is also evaluated by simulation results.

1.2 Reliable Low-Energy Group Formation for Infrastructureless Public Safety Networks

The current technology standards for PSNs, such as TETRA, TETRAPOL, and DMR, provide terrestrial radio access technologies using direct communications between de-

vices when base stations and wired backbone lines are not operational in emergency situations as shown in Fig. 1.1 [14, 7, 3]. To utilize unprecedentedly rapid advances in commercial wireless networks, the 3rd Generation Partnership Project Long-Term Evolution (3GPP LTE) has recently been adopted as a baseline platform for the next generation PSNs in the United States, and South Korea. 3GPP standardization body has been evolving LTE specifications to support direct communication between UEs in out-of-coverage [15, 16, 17]. To this end, recent evolution of 3GPP LTE has introduced group owner mode to enable public safety networks [18]. The group owner mode is a key feature for direct communications between UEs especially in infrastructure-less PSN (IPSN) where data transfer via infrastructure is unavailable. Some UEs are designated as group owners (GOs) in the group owner mode and are responsible for group formation, communication with their group members (GMs), and inter-group routing as a wireless backbone. Each non-GO UE becomes a GM of its proximate group by performing authentication with the GO of the group. The benefits from the group-based hierarchy in IPSN include better scalability, bandwidth reuse, and simple routing [19]. However, efficient group formation methods have not been fully studied.

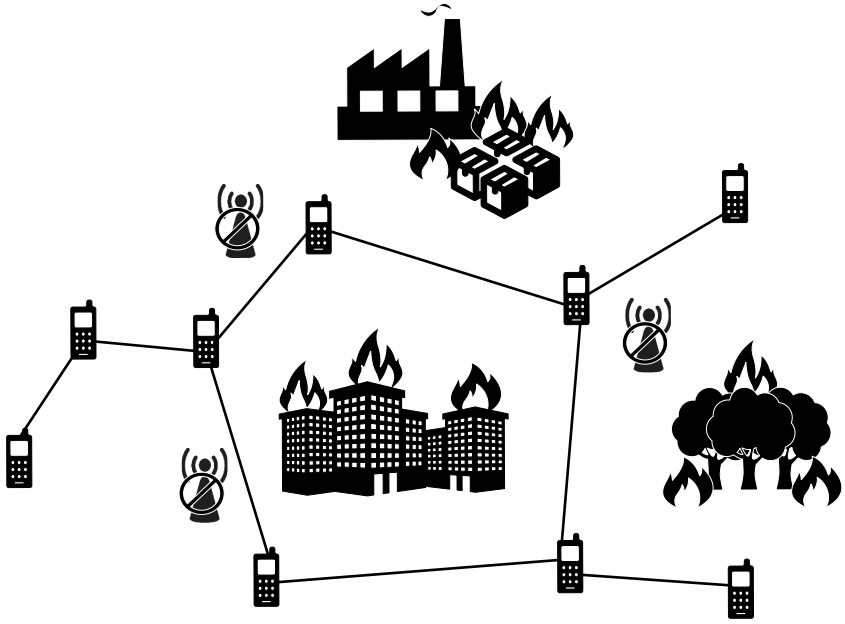

Figure 1.1: Overview of an infrastructure-less public safety network.

In this dissertation, we focus on two critical goals to organize groups for PSNs: energy efficiency and reliability. IPSNs should minimize energy consumption of UEs to maximize the survival time of the networks. In addition, IPSNs should guarantee reliable communications. In order to guarantee reliable communications, any pair of UEs should be connected through only qualified links considering wireless coverage. These goals are extremely important in IPSNs, as failing to meet the goals could directly lead to losses of lives or property. The previous studies have investigated minimizing the total energy of the network in wireless sensor networks (WSNs) [20, 21, 22, 23, 24, 25] . In WSNs, low-energy adaptive clustering hierarchy-centralized (LEACH-C) [22] proposed a pioneering idea, which minimizes the total energy consumption of the network using a clustered hierarchy. In LEACH-C, simulated annealing-based optimization algorithm [26] is adopted for cluster formation. Several improvements have been proposed to enhance LEACH-C by considering residual energy[23], a re-clustering frequency[24], and solar cells[25]. In [27, 28, 29], LEACH-C has been improved by replacing simulated annealing with K-means clustering [30], which has been proved to be efficient for most clustering tasks in machine learning fields. Recent studies have developed network formation techniques based on game theory [31, 32, 33, 34, 35, 36]. Among various studies exploiting coalition game for communications networks, study in [31] proposed a hybrid homogeneous LEACH protocol (HHO-LEACH) to minimize energy consumption of the network. As described in its name, HHO-LAECH is based on LEACH in minimizing energy consumption. However, the connectivity constraints are not considered in [31] like other studies that have enhanced LEACH. Network formation under connectivity constraint has been focusing on connected dominating set (CDS) [37, 38, 39, 40]. In graph theory, CDS is defined as a connected subgraph of a graph to which every vertex not belonging to the CDS is adjacent. For the last two decades, various algorithms such as Guha and Khuller's algorithm and Ruan's algorithm have been developed for various types of CDS constructions [41, 42]. In ad-hoc networks, a CDS is used to select a wireless backbone network guaranteeing reliable

connection for routing and control [37, 38, 39, 40]. Vertices and edges in a graph represent the set of nodes and the set of links in ad-hoc network, respectively. Whether any pair of nodes are adjacent to each other or not (that is, whether two vertices are connected by an edge in a graph) depends on the distance between them. The aforementioned studies cannot be directly applied to IPSNs because they focus on either minimizing the total energy consumption or guaranteeing reliable connection. Clustering algorithms that minimize total energy consumption do not consider connectivity constraints for reliable communication between UEs. On the other hand, minimization of total energy consumption of a network is not considered in the CDS-based network formation techniques. Thus, we propose a new network formation scheme for IPSN considering both minimizing total energy consumption and guaranteeing reliable communications.

To resolve the challenges, we formulate a constrained clustering problem for group formation of IPSNs considering both energy efficiency and reliability. Our formulation becomes mixed integer programming which requires a combinatorial optimization. We propose a low-complexity clustering algorithm to solve this problem. As will be discussed in detail in the next section, existing techniques are not efficient enough to provide a satisfactory solution to the problem, thus motivating us to introduce affinity propagation (AP) [9], a state-of-the-art message-passing technique. AP has been proven to be a very efficient tool for various types of optimization problems in communication networks [43, 10, 12]. The proposed clustering algorithm based on the AP framework efficiently minimizes the total energy consumption of IPSNs while guaranteeing reliable communications.

Our main contributions are summarized as follows:

- **IPSN organization:** We formulate the IPSN group formation as a *constrained* clustering problem. Unlike the conventional clustering problems studied in the literature, our clustering formulation minimizes energy consumption while guaranteeing reliable communications. This requires a computationally demanding

optimization.

- **Low-complexity algorithm:** We propose a low-complexity clustering algorithm for the constrained clustering problem in the AP framework. The proposed clustering algorithm iteratively performs AP to determine the number of clusters adaptively. In addition, we present how to determine initial parameters to reduce the number of required iterations and improve the convergence speed.

- **Energy-saving performance:** Our simulation results verify that the proposed clustering algorithm reduces the total energy consumption in the network by up to 31% compared to the conventional clustering algorithms. Note that such energy saving is achieved while guaranteeing reliable communication in the network.

1.3 Outline of Dissertation

The remainder of this dissertation is organized as follows. In Chapter 2, we propose a distributed synchronization algorithm based on message-passing and the procedures for distributed synchronization. The proposed grouping algorithm is compared with the synchronization algorithm by simulation results. In Chapter 3, we propose a novel clustering algorithm in the AP framework. How to determine the initial parameter $p^{(1)}$ is presented to reduce the number of iterations required by the proposed clustering algorithm. The simulation results show the proposed grouping algorithm outperforms the conventional algorithms. In Chapter 4, conclusions are drawn and future research topics are discussed.

1.4 Notations

$\max(x, y)$ denotes the maximum of x and y. $\min(x, y)$ denotes the minimum of x and y. $\lceil x \rceil$ is used to refer to the smallest integer not less than x. $|x|$ is the absolute

value of a real number x. $|\mathcal{A}|$ denotes the cardinality of a set $\mathcal{A}$. The same notation is used to refer to the absolute value and the cardinality, and the meaning depends on the input of the operator. $\mathbb{E}[\cdot]$ denotes the expected value of a random variable. $\mathbb{P}[\cdot]$ denotes the probability of an event occurring. A summary of the notations frequently used in Chapter 2 is listed in Table 1.1 and a summary of the notations frequently used in Chapter 3 is listed in Table 1.2

Table 1.1: Frequently used notations in Chapter 2

Notation	**Definition**
N	Number of UEs
$\mathcal{V}$	Set of SyncRef UEs
$\mathcal{N}_j$	Set of non-SyncRef UEs associated with SyncRef j
P	Transmit power of synchronization signals
d_{ij}	Distance between UE i and UE j
$s(i,j)$	Similarity of UE i to UE j

Table 1.2: Frequently used notations in Chapter 3

Notation	**Definition**
N	Number of UEs
$\mathcal{V}$	Set of GOs
$\mathcal{N}_j$	Set of GMs associated with GO j
d_{ij}	Distance between UE i and UE j
r_1	Maximum range for reliable intra-group link
r_2	Maximum range for reliable inter-group link
$w(d_{ij})$	Power consumption for the transmission between GO j and UE i
$\bar{w}$	Power consumption for the management of each group
$s(i,j)$	Similarity of UE i to UE j

Chapter 2

Distributed Synchronization Algorithm for Infrastructure-less Public Safety Networks

2.1 System Model and Problem Formulation

We consider an IPSN composed of N UEs. A subset of UEs become SyncRef UEs and periodically broadcast synchronization signals. The other UEs, referred to as non-SyncRef UEs, detect synchronization signals and select the strongest one as their synchronization reference. Fig. 3.1 illustrates synchronization of IPSNs, where the black UEs, white UEs, border lines, and arrows denote the SyncRef UEs, non-SyncRef UEs, SyncGroups, and broadcasting synchronization signals, respectively. We assume a low-rate control channel to exchange information for SyncRef selection among neighboring UEs without prior synchronization. This can be implemented by embedding synchronization information in every transmitted data packet. One example of this type of channel is a physical sidelink broadcast channel (PSBCH) defined in 3GPP-LTE Rel-12 [44]. PSBCH does not have a mechanism to prevent a collision problem. Hence, collisions may occur in control channels, and messages in the control channels may not be received correctly. Note that the proposed algorithm is robust to partial loss of message. The impact of control channel collisions on the proposed algorithm

is evaluated in Section 2.4.

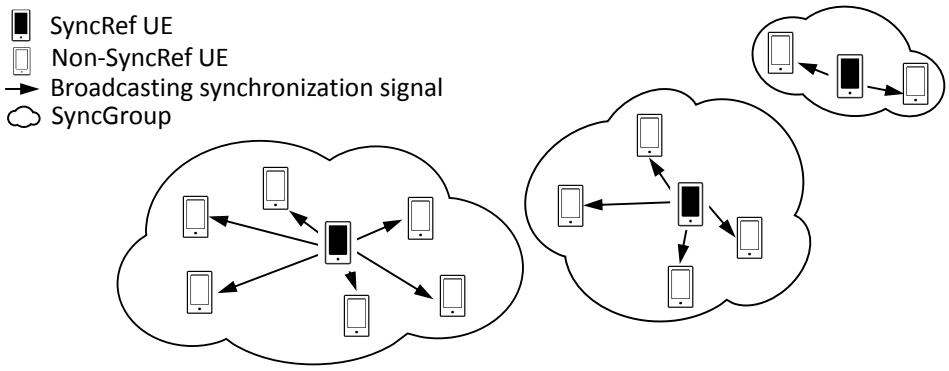

Figure 2.1: Synchronization of infrastructure-less public safety networks.

Assuming UE j as a candidate SyncRef UE of UE i, the received power of a synchronization signal at UE i is given by

$$P_{\text{rx}}(i) = PX_{ij}L_0\left(\frac{d_{ij}}{d_0}\right)^{-\alpha}, \tag{2.1}$$

where P, X_{ij}, L_0, d_{ij}, d_0, and α denote the transmit power, the fading coefficient between UE i to UE j, the path-loss at the reference distance d_0, the distance between UE i and UE j, the reference distance, and path-loss exponent, respectively. We assume that the period of the synchronization signals, T_s, is greater than the coherence time of the channel. Then, X_{ij} is considered an independent random variable.

The detection of a synchronization signal is assumed to fail if the received signal-to-noise-ratio (SNR) of a synchronization signal is below a threshold γ, which is a minimum SNR required for the successful detection. The success of a synchronization signal detection is probabilistic due to channel fluctuations. The probability of a single failure of the synchronization signal detection at UE i, denoted by q_i, is

$$q_i = \mathbb{P}\left[\frac{P_{\text{rx}}(i)}{\sigma^2} < \gamma\right], \tag{2.2}$$

where σ^2 represents the noise power. For Rayleigh fading, where X_{ij} is exponentially distributed with unit mean, the failure probability is derived as [45]

$$q_i = 1 - \exp\left(-\frac{1}{2}\left(\frac{\gamma\sigma^2 d_{ij}^{\alpha}}{PL_0 d_0^{\alpha}}\right)^2\right). \tag{2.3}$$

Fig. 2.2 depicts an example of the synchronization procedures. A single detection failure of a synchronization signal does not immediately lead to an out-of-sync state. A UE falls into an out-of-sync state if detection failures continue for the maximum endurance time of T_{max}. The value of T_{max} is a system-defined parameter and is carefully determined considering the hardware requirements for the UE oscillators [6]. Thus, after $M = \lceil T_{\text{max}}/T_s \rceil$ consecutive failures of the synchronization signal detection, a

UE falls into an out-of-sync state. The UE returns into an in-sync state after any single successful detection of the synchronization signal. The probability that UE i remains in an out-of-sync state is $p_i = q_i^M$.

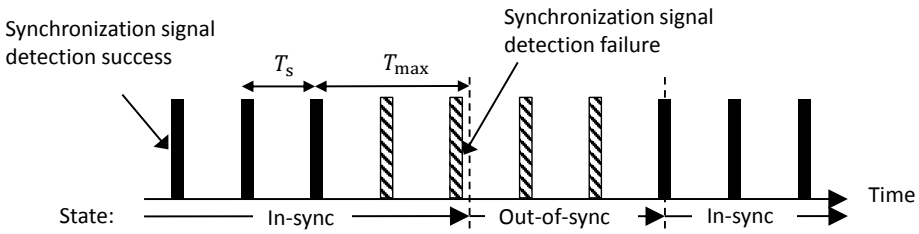

Figure 2.2: Example of synchronization procedures.

We refer to UEs that are in an out-of-sync state and thus experience RLF as out-of-sync UEs hereafter. The number of out-of-sync UEs is the sum of the random variables Y_i's, where Y_i denotes the out-of-sync state of UE i. The random variable Y_i follows a Bernoulli distribution taking a value of '1' with probability p_i, and a value of '0' otherwise. The average number of out-of-sync UEs can be computed as follows:

$$\begin{aligned}\bar{N}_{\text{out}} &= \mathbb{E}\left[\sum_{i=1}^{N} 1 \cdot Y_i\right] \\ &= \sum_{i=1}^{N} \mathbb{E}\left[Y_i\right] \\ &= \sum_{i=1}^{N} p_i \\ &= \sum_{i=1}^{N} \left[1 - \exp\left(-\frac{1}{2}\left(\frac{\gamma\sigma^2 d_{ij}^{\alpha}}{PL_0 d_0^{\alpha}}\right)^2\right)\right]^M .\end{aligned} \tag{2.4}$$

Then, the selection of the SyncRef UEs that minimizes the number of out-of-sync UEs can be formulated as

$$\text{minimize} \sum_{j\in\mathcal{V}} \sum_{i\in\mathcal{N}_j} \left[1 - \exp\left(-\frac{1}{2}\left(\frac{\gamma\sigma^2 d_{ij}^{\alpha}}{PL_0 d_0^{\alpha}}\right)^2\right)\right]^M , \tag{2.5}$$

where $\mathcal{V}$ and $\mathcal{N}_j$ are the set of SyncRef UEs and the set of non-SyncRef UEs associated with SyncRef UE $j \in \mathcal{V}$, respectively. Note that the problem in (2.5) belongs to an integer programming typically requiring combinatorial optimization with exponentially growing computational complexity.

2.2 Distributed Synchronization Algorithm based on Message-passing

2.2.1 Preliminaries: affinity propagation

AP is a state-of-the-art clustering algorithm developed in computer science based on a message-passing algorithm [9, 47]. It was originally proposed to find a set of representative data points (or exemplars) to partition a set of data points into subsets of data points. AP has various advantages. First, it outperforms existing clustering algorithms, i.e., K-means clustering and simulated annealing. Secondly, AP provides a deterministic result, unlike other clustering algorithms whose performance depends on the choice of the initial point. Thirdly, AP can be adapted to various complicated problems owing to its flexibility.

The inputs of AP are the real-valued similarities, and the objective of AP is to select GOs which maximize the sum of similarities as formally described by

$$\text{maximize} \sum_{j \in \mathcal{V}} \sum_{i \in \mathcal{N}_j} s(i,j), \tag{2.6}$$

where $s(i,j)$ denotes the similarity of UE i to UE j. The similarity $s(i,j)$ of UE i indicates the suitability of UE j to be the GO of UE i. The preference (or self-similarity) $s(j,j)$ of UE j indicates the suitability of UE j to be a GO. AP considers all UEs as potential GOs and selects GOs by passing messages iteratively between the UEs. Two types of messages are defined in earlier work [9] as *responsibility* and *availability*. After each iteration of passing messages, the messages are updated by the update rule derived in [9, 47] based on the max-sum algorithm in a factor graph. The message of responsibility $r(i,j)$ from UE i to potential GO j reflects the accumulated evidence about the suitability of UE j serving as the GO for UE i, considering other potential GOs for UE i. The initial value of responsibility is set to $r(i,j) = s(i,j) - \max_{j' \text{s.t.} j' \neq j} s(i,j')$. The update rule of the responsibility $r(i,j)$ from UE i to potential

GO j is

$$r(i,j) = s(i,j) - \max_{j' \text{s.t.} j' \neq j} \Big\{ a(i,j') + s(i,j') \Big\}. \tag{2.7}$$

The availability $a(i,j)$ from the potential GO j to UE i reflects the accumulated evidence about the suitability choosing UE j as the GO of UE i, considering the support from other UEs that UE j should be a GO. The initial value of availability is set to $a(i,j) = 0$. The update rule of the availability $a(i,j)$ from potential GO j to UE i is

$$a(i,j) = \min \Big(0 \ , \ r(j,j) + \sum_{i' \text{s.t.} i' \notin \{i,j\}} \max \big(0, r(i',j)\big) \Big). \tag{2.8}$$

The self-availability of UE j reflects the accumulated evidence about UE j being a GO, considering the positive responsibilities sent to candidate GO j from other UEs. The initial value of availability is also set to $a(j,j) = 0$. The self-availability of UE j is updated differently with the availability $a(i,j)$ as

$$a(j,j) = \sum_{i' \text{s.t.} i' \neq j} \max \big\{ 0, r(i',j) \big\}. \tag{2.9}$$

Messages are exchanged iteratively until the fixed number of iterations is reached, or the decision of the GOs remains unchanged for the fixed number of iterations. After termination of message exchanges, the GO $j^\star$ of UE i is determined as

$$j^\star = \arg\max_j \Big\{ a(i,j) + r(i,j) \Big\}, \tag{2.10}$$

if $j^\star \neq i$. UE i itself becomes a GO if $j^\star = i$.

The overall computational complexity of affinity propagation increases as $\mathcal{O}(N \bar{N} t_{\max})$, where $\bar{N}$ denotes the average number of UEs adjacent to a UE and $t_{\max}$ denotes the maximum number of iterations. Decades of iterations are enough to converge in AP [11, 12] and the convergence properties and proofs are discussed in depth in [11, 12]. Another advantage of this approach is that the computational load of affin-

ity propagation can be implemented in a distributed fashion using multi-core processors [48]. Although the renewal periods of clusters depend on the mobility patterns of UEs, clusters organized by the proposed algorithm are expected to be maintained for a few minutes without a renewal of the clusters. Considering that the proposed clustering algorithm is performed on a long-term time scale, the computation cost for the proposed clustering algorithm is manageable.

2.2.2 Distributed Synchronization Algorithm

Motivated by the analogy between our problem in (2.5) and AP in (2.6), we derive solutions by applying the AP framework to our problem. We define the similarity between UE i and UE j ($i \neq j$) as

$$s(i,j) = -\left[1 - \exp\left(-\frac{1}{2}\left(\frac{\gamma\sigma^2 d_{ij}^{\alpha}}{PL_0 d_0^{\alpha}}\right)^2\right)\right]^M. \tag{2.11}$$

With the above similarity definitions, maximizing the sum similarities in (2.6) becomes equivalent to minimizing the number of out-of-sync UEs in (2.5). The self-similarity (or preference) of each UE ($i = j$) is defined as

$$s(j,j) = \begin{cases} p, & \text{if UE } j \text{ is eligible as a SyncRef,} \\ -\infty, & \text{otherwise,} \end{cases} \tag{2.12}$$

where p is defined as a negative value. A pre-defined parameter p affects the number of UEs selected as SyncRef during SyncRef selection. We can exclude UEs with high mobility, or low residual energy from becoming SyncRef UEs by setting their preferences to $-\infty$.

The proposed algorithm is presented in Algorithm 1, where t denotes the iteration index and $t_{\max}$ denotes the maximum number of iterations. The algorithm starts by initializing messages as $a(i,j) = 0$ and $r(i,j) = s(i,j) - \max_{j' \text{s.t.} j' \neq j} s(i,j')$. Each UE

Algorithm 1 Proposed Synchronization Algorithm

Initialization: $a(i,j) \leftarrow 0, r(i,j) \leftarrow s(i,j), t \leftarrow 1$
while $t \leq t_{\max}$ & not converge **do**
    Each UE updates $r(i,j)$ using (2.7)
    Each UE updates $a(i,j)$ using (2.8) and (2.9)
    Send $a(i,j)$ & $r(i,j)$ to neighboring UEs
    $t \leftarrow t+1$
end while
Decision: Each UE determines its SyncRef using (2.13)

continues to exchange "Responsibility" and "Availability" messages with neighboring UEs. During message exchanges, UE i updates availability $a(j,i)$ using (2.7) and updates responsibility $r(i,j)$ using (2.8) and (2.9) for neighboring UE j. At the beginning of each iteration, UEs check the termination condition. If the termination condition is satisfied, each UE autonomously determines whether to become a SyncRef or not. UE i computes its best SyncRef $j^\star$ as

$$j^\star = \arg\max_j \left[a(i,j) + r(i,j)\right]. \tag{2.13}$$

If $j^\star \neq i$, UE $j^\star$ becomes a SyncRef of UE i while UE i becomes a SyncRef itself if $j^\star = i$.

The overall computational complexity of the proposed synchronization algorithm increases as $\mathcal{O}(K^2 t_{\max})$, where K denotes the average number of neighboring UEs. In the proposed algorithm, each UE is responsible for updating its own messages. Thus, the computational burden on each UE is simply $\mathcal{O}(K t_{\max})$, which is manageable considering that the number of neighboring UEs for a single UE is limited.

2.3 Distributed Synchronization Procedures

The distributed synchronization procedures consist of four phases. Fig. 2.3 illustrates an example of distributed synchronization of two UEs. In Phase I, UEs discover their neighbors. Each UE broadcasts a "Hello" message containing its identity information

and a reference signal to announce its existence. By decoding received “Hello” messages, UEs identify their neighbors. In addition, UEs estimate the distances to their neighbors by measuring the received power of the reference signal or by exchanging position information based on GPS in “Hello” messages. Each UE creates its neighbor list consisting of the identities of neighboring UEs and similarities between itself and them. In Phase II, UEs exchange messages with their neighbors according to the distributed synchronization algorithm described in Algorithm 1. Upon the termination of the algorithm, SyncRef UEs are selected. In Phase III, SyncGroups are formed. UEs selected to become SyncRef UEs announce their IDs through “SyncRef Notification” messages. Non-SyncRef UEs wait for “SyncRef Notification” messages from neighboring SyncRefs. When a “SyncRef Notification” message is detected, non-SyncRef UEs are synchronized to the SyncRef. If multiple “SyncRef Notification” messages are detected, the SyncRef with the strongest received power is selected. In Phase IV, typical data communication continues. SyncRef UEs in each SyncGroup periodically transmit synchronization signals for their members. Non-SyncRef UEs synchronize to the SyncRef UE with the strongest received power. Overall synchronization procedure is repeated with a predetermined period.

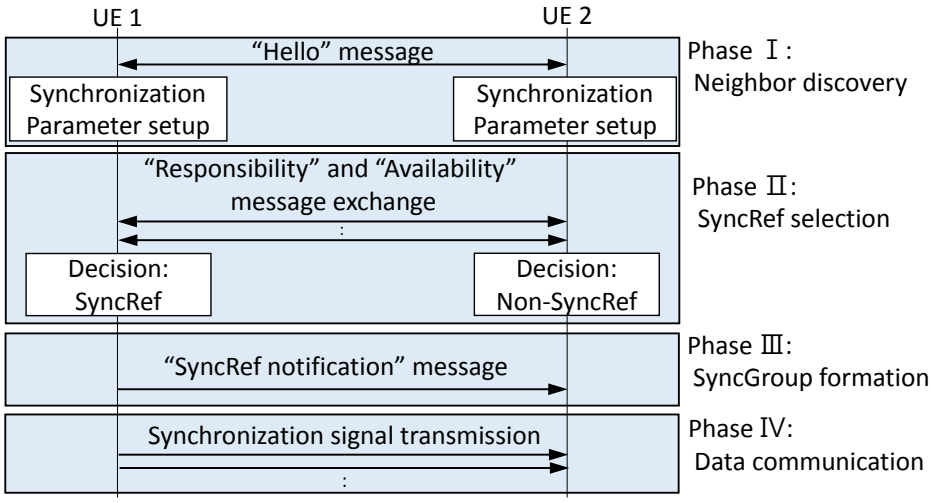

Figure 2.3: Example of distributed synchronization with two UEs.

When a UE first joins the network, it should wait until the start of the next round of synchronization procedure. A UE participates in the on-going synchronization procedure if a synchronization procedure is detected, i.e., by listening to "Hello" messages. If it fails to detect any synchronization procedure for more than a predetermined period, the UE initiates a synchronization procedure itself. Accordingly, UEs that join the IPSN are sequentially associated with synchronization procedures. Fig. 2.4 illustrates a detailed example of the UE's behavior related to the initiation and termination of the SyncRef selection, where T_i denotes a pre-configured period to repeat SyncRef selection procedures periodically. When the first UE, named UE-1, joins the PSN, no synchronization procedure is detected during an interval T_i. Thus, UE-1 initiates a synchronization procedure after T_i. If UE-2 joins the PSN, UE-2 detects the initiation of synchronization procedures from UE-1 within T_i. Then, UE-2 starts to exchange messages to select SyncRef UE as described in Fig. 2.4. UE-1 and UE-2 periodically repeat synchronization procedures at the same timing. Similarly, UE-3 can join the PSN, and get involved in the synchronization procedure successfully.

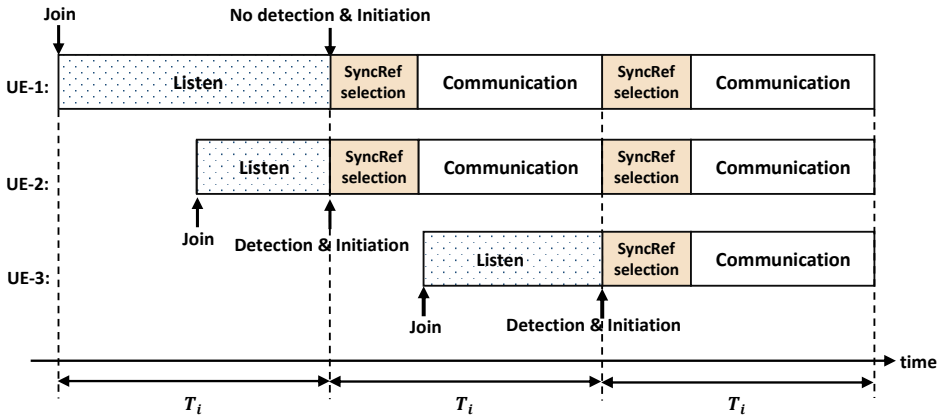

Figure 2.4: Example of synchronization procedures with three UEs.

2.4 Simulation Results

The proposed algorithm is evaluated through extensive simulations. A square area of 5 km $\times$ 5 km is considered. We adopt the WINNER+ B1 path-loss model with $\alpha = 4.37$ and $L_0 = 0.068$ at a height of 1.5 m and a carrier frequency of 700 MHz [17, 49], which is the most preferred spectrum for public safety purpose globally. A transmit power of $P = 32$ dBm, and a noise power of $\sigma^2 = -104$ dBm are considered. We consider two SNR thresholds to detect a synchronization signal successfully: $\gamma = -6$ dB as an optimistic setting and $\gamma = 0$ dB as a conservative setting. UEs are considered to fall into an out-of-sync state after failing to detect a synchronization signal in the case of $M = 1$. To evaluate performance with the varying number of SyncRef UEs, the preference which decides the number of SyncRef UEs is controlled in $[-10, -0.1]$. The message-passing algorithm terminates when the number of iterations reaches $t_{\max} = 100$ or when messages remain unchanged for 10 iterations. The performances are averaged over 100 independent realizations of user distributions.

Table 2.1: Simulation parameters

Parameter	**Value**
Area, S	5 km $\times$ 5 km
Number of UEs, N	1000, 750, 500
Pathloss exponent, α	4.37
Transmission loss at $d_0 = 1$ m, L_0	0.068 dB
Noise power, σ^2	-104 dBm
Transmit power for a synchronization signal, P	32 dBm
SNR threshold to detect a synchronization signal, γ	-6 dB, 0 dB

Fig. 2.5 and Fig. 2.6 compares the average numbers of out-of-sync UEs in the proposed algorithm and in the scan-and-select strategy as a function of the number of SyncRefs when the number of UEs is $N = 1000$, 750, and 500 and the SNR threshold is $\gamma = -6$ dB and $\gamma = 0$ dB. As the number of SyncRef UEs (and SyncGroups) increases, the average number of out-of-sync UEs decreases because the average distance to SyncRef UEs decreases. We observe that the proposed algorithm outperforms

the scan-and-select strategy in various environments. The proposed algorithm reduces the average number of out-of-sync UEs by up to 38.7% and 40.4% compared to the scan-and-select strategy when $\gamma = -6$ dB. In other words, to achieve the same out-of-sync performance, 27% more UEs should be selected as SyncRef UEs in the scan-and-select strategy. This indicates that the proposed algorithm can significantly reduce the unnecessary power consumption, signaling overhead, and potential interference in the network. The performance gain of the proposed algorithm stems from local information sharing between neighboring UEs for the collaborative optimization of SyncRef and SyncGroup determination.

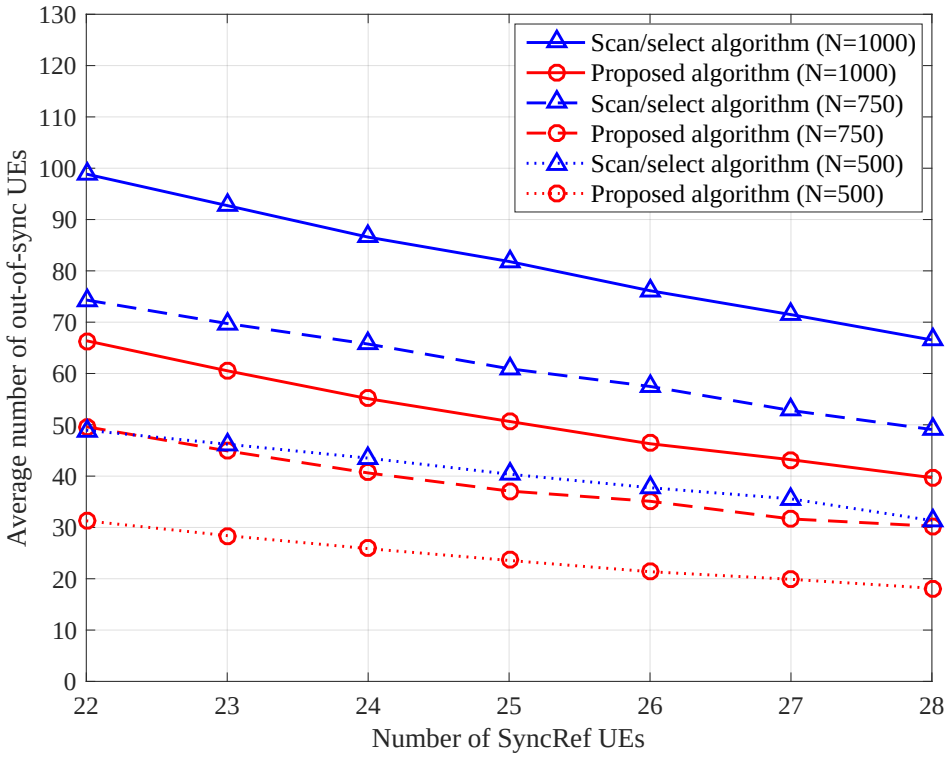

Figure 2.5: Average number of out-of-sync UEs versus the number of SyncRefs for $\gamma = -6$ dB case.

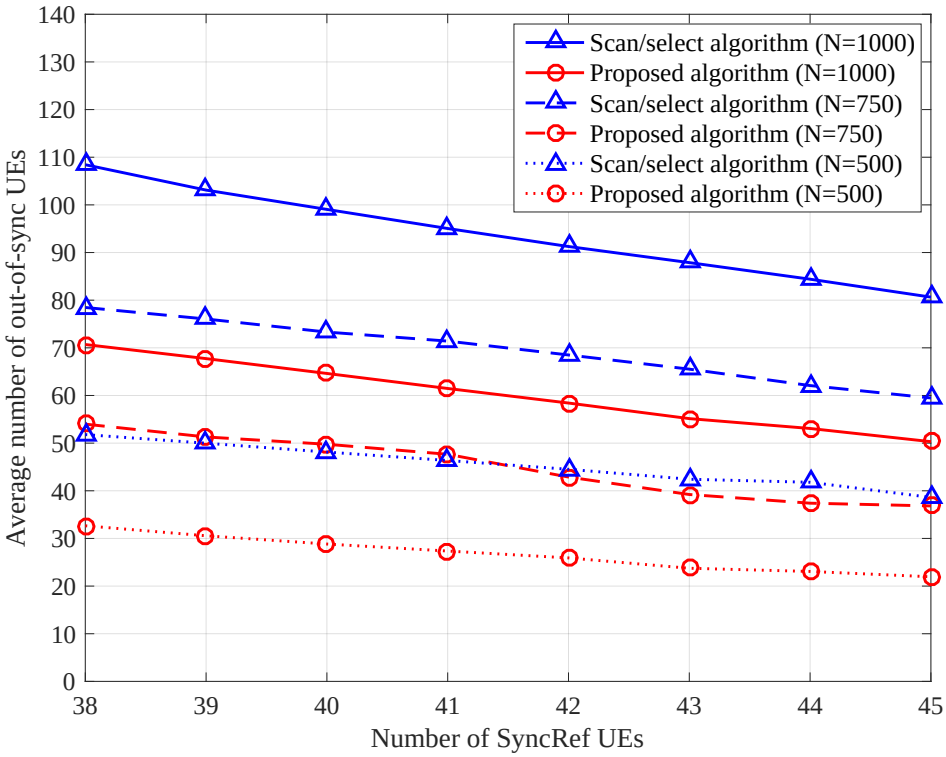

Figure 2.6: Average number of out-of-sync UEs versus the number of SyncRefs for $\gamma = 0$ dB case.

Fig. 2.7 compares the empirical cumulative distribution function (CDF) of the number of asynchronous timings in the proposed algorithm and the scan-and-select strategy when $N = 1000$. The number of asynchronous timings is defined as the number of SyncRefs that a UE should keep tracking to successfully decode received signals from its neighboring UEs [50]. Typically, fewer asynchronous timings are preferred for UEs because tracking multiple asynchronous timings increases hardware complexity and power consumption of UEs. For a fair comparison, we consider cases with similar out-of-sync performance, i.e., 22 SyncRef UEs for the proposed algorithm and 28 SyncRef UEs for the scan-and-select strategy when $\gamma = -6$ dB, and 38 SyncRef UEs for the proposed algorithm and 45 SyncRef UEs for the scan-and-select strategy when $\gamma = 0$ dB, as shown in Fig. 2.5 and Fig. 2.6. Specifically, if we limit the number of asynchronous timings to two, 69% of UEs can communicate with all their neighbors in the proposed algorithm while only 51% of UEs can communicate with all their neighbors in the scan-and-select strategy.

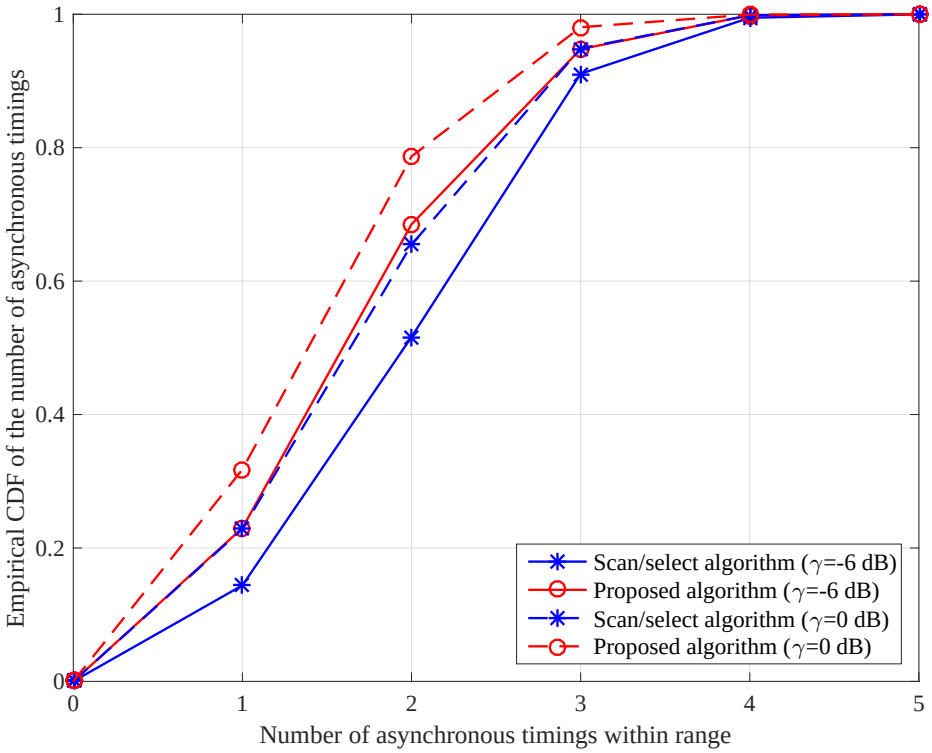

Figure 2.7: CDF of the number of asynchronous timings when $N = 1000$.

Fig. 2.8 shows the average number of out-of-sync UEs versus the message exchange failure probability in control channels, when the number of UEs is $N = 1000$. Case 1 considers $\gamma = -6$ dB and 22 SyncRef UEs, Case 2 considers $\gamma = -6$ dB and 28 SyncRef UEs, Case 3 considers $\gamma = 0$ dB and 38 SyncRef UEs, and Case 4 considers $\gamma = 0$ dB and 45 SyncRef UEs. The results show the impact of the failure of message exchanges on a SyncRef selection in the proposed algorithm. The message exchange failure probability, denoted by p_e, is defined as the probability that a message is not received correctly in control channels. As the message exchange failure probability increases, the average number of out-of-sync UEs gradually increases. For $p_e \leq 0.5$, the proposed algorithm still notably outperforms the scan-and-select strategy for the same cases shown in Fig. 2.5 and Fig. 2.6. The proposed algorithm gradually updates messages based on message-passing and still converges regardless of partial loss of messages in control channels. If the message loss surpasses a system endurance level, e.g., $p_e > 0.5$ in Fig. 2.8, the proposed algorithm fails to converge, leading to considerable performance degradation. However, this can be considered an extreme case. The simulation results imply that the proposed algorithm can be implemented with a control channel of PSBCH defined in 3GPP-LTE in the presence of potential collision probability.

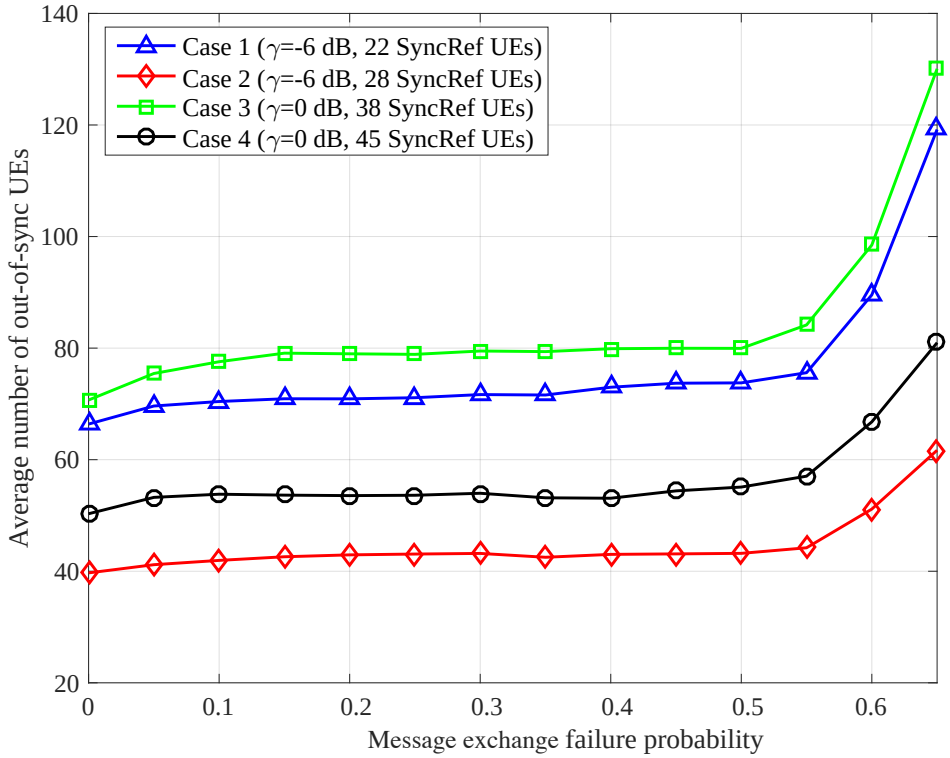

Figure 2.8: Average number of out-of-sync UEs versus the message exchange failure probability.

Table 2.2 shows how the average number of out-of-sync UEs varies with the number of iterations in the proposed algorithm. Case A considers $N = 1000$, $\gamma = -6$ dB, and 22 SyncRef UEs, Case B considers $N = 1000$, $\gamma = 0$ dB, and 38 SyncRef UEs, and Case C considers $N = 500$, $\gamma = -6$ dB, and 22 SyncRef UEs. In general, larger number of iterations improves the performance of the proposed algorithm. However, the algorithm complexity can be considerably reduced by slightly sacrificing the performance. Note that the proposed algorithm with $t_{\max} = 20$ still notably outperforms the scan-and-select strategy. Extensive simulation studies have shown that a small number of iterations typically suffices convergence in the AP framework [11]. More details on the convergence properties and proofs can be found in [12] and references therein. Considering that periodic renewals of SyncRefs are performed on a long-term time scale, signaling overhead and computational cost required for the proposed algorithm are manageable.

Table 2.2: Average number of out-of-sync UEs vs number of iterations

	Proposed algorithm					Scan/select algorithm
# of iterations	20	40	60	80	100	
Case A	69.4	68.0	67.1	66.9	66.4	98.9
Case B	72.1	71.2	71.2	70.7	70.1	108.4
Case C	31.5	31.2	31.2	31.1	31.0	49.0

Fig. 2.9 shows the empirical CDF of the SyncRef UEs with uniformly distributed residual battery energy where $\gamma = -6$ dB, and $N = 500$. We set the preference of UE j as $s(j, j) = p_0/E_j$, where p_0 denotes the preference of UEs with fully-charged battery, and E_j denotes the residual energy of UE j's battery in percent. The value of p_0 is a system parameter which should be less than zero and is determined with the density of SyncRef UEs in IPSN. We set the value of preference of UEs with fully-charged battery as $p_0 = -4$ in Fig. 2.9. By this setting, UEs with higher percent of battery set their preference as higher value and are more likely to be a SyncRef UE as shown in Fig. 2.9. UEs with battery energy less than 70% are rarely selected as SyncRef

UE in the proposed algorithm. Syncref UEs additionally consume energy to transmit synchronization signals and the preference setting helps UEs with low residual energy prolong battery lifetimes of the UEs.

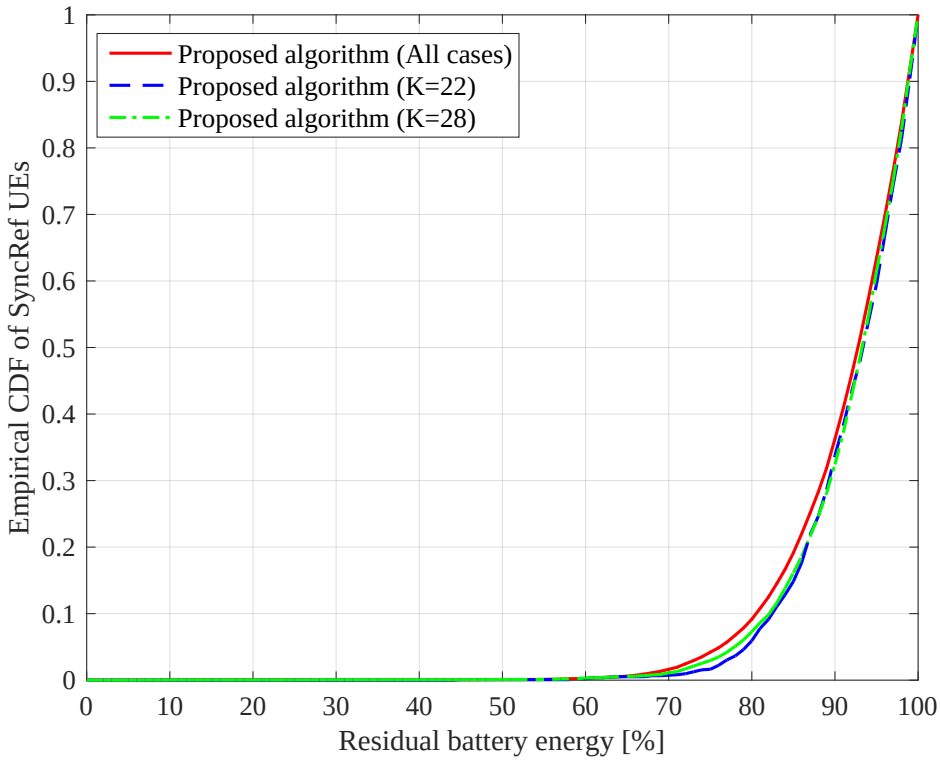

Figure 2.9: Empirical CDF of the number of SyncRef UEs with uniformly distributed residual battery energy where $\gamma = -6$ dB, and $N = 500$.

Fig. 2.10 shows average number of out-of-sync UEs in the proposed clustering algorithm as a function of time and UE speed, denoted by v, where $\gamma = -6$ dB, 23 SyncRefUEs, and $N = 500$. A random walk model [57], one of the most widely employed model in ad-hoc network [58] and sensor network [59], is used for UEs' mobility pattern. After the proposed algorithm selects SyncRef UEs to minimize the average number of out-of-sync UEs, the average number of out-of-sync UEs increases due to the mobility. As UEs move faster, the number of out-of-sync UEs increases rapidly and the SyncRef selection procedures should be performed more frequently to maintain reliable synchronizations. However, with the repetition of SyncRef selection procedures every 10 minutes, the increase of the average number of out-of-sync UEs remains less than 15% percent when UEs move at the speed of $v = 12$ km/h. Even in the case that all UEs are stationary, the SyncRef selection procedures should be periodically performed to reflect the changes in IPSN caused by UEs' joining and leaving. Thus, a pre-configured period to repeat SyncRef selection procedures can be set as $T_i = \min(T^{\mathrm{X}}, T_{i,\mathrm{min}})$, where T^{X} denotes the maximum time interval in which the increase of the average number of out-of-sync UEs is less than X percent, and $T_{i,\mathrm{min}}$ is the minimum period interval to repeat SyncRef selection procedures.

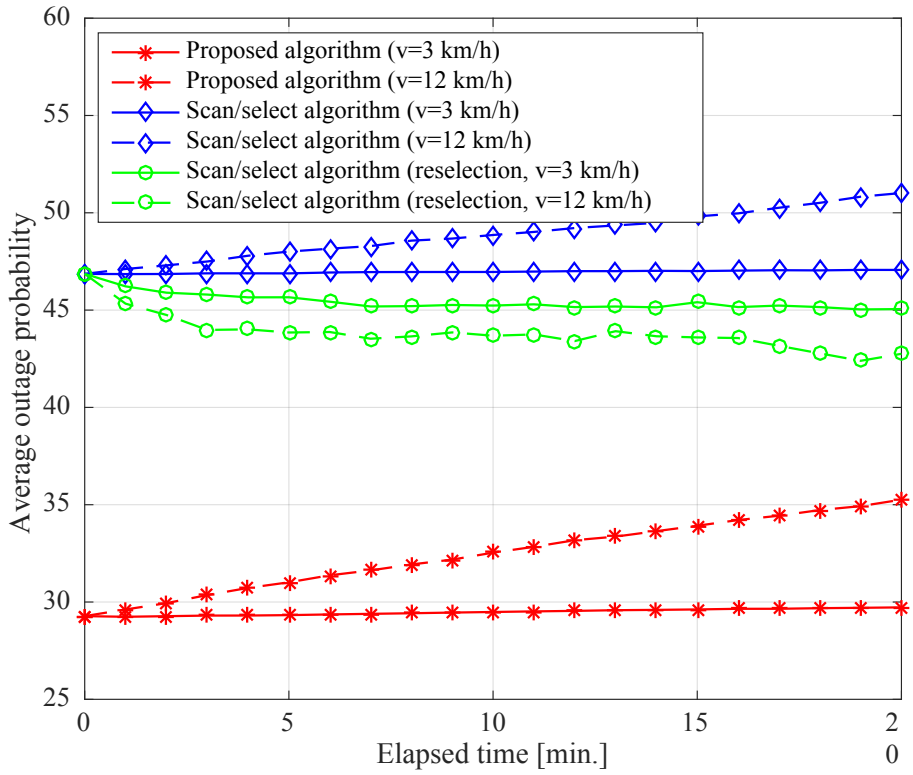

Figure 2.10: Average number of out-of-sync UEs versus elapsed time where $\gamma = -6$ dB, 23 SyncRef UEs, and $N = 500$.

Fig 2.11 shows the average number of out-of-sync UEs as a function of parameter M which denotes the number of consecutive synchronization failures to fall into out-of-sync state. Because M is an exponent in the problem formulation 2.12, the average number of out-of-sync UEs for larger M is much less than that for smaller M in both of the proposed algorithm and scan-and-select algorithm. The increase of M by one results in reduction of the average number of out-of-sync UEs by up to 77%. For all values of M, the proposed algorithm shows smaller number of out-of-sync UEs than scan-and-select algorithm.

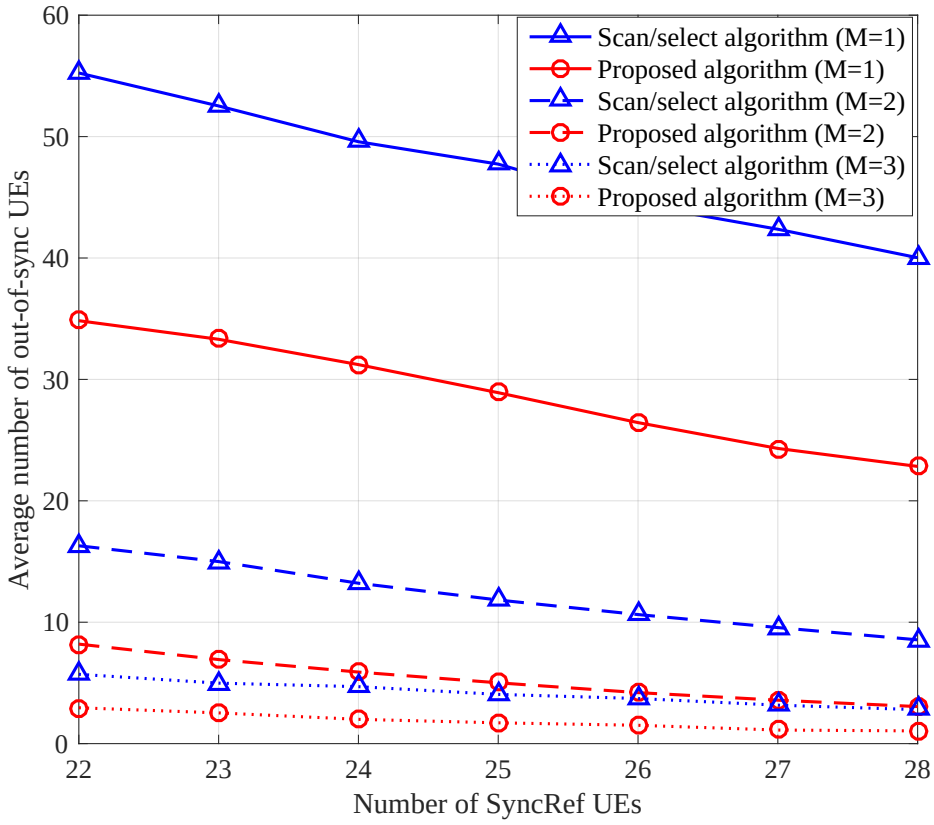

Figure 2.11: Average number of out-of-sync UEs versus the number of SyncRefs where $M = 1$, 2, and 3, and $N = 500$.

Fig. 2.12 shows how the average number of out-of-sync UEs varies with the number of quantization bits of messages, N_q, where $\gamma = -6$ dB, 23 SyncRef UEs, and $N = 500$. The availability messages and responsibility messages should be quantized before being transmitted to neighboring UEs and for more practical scenarios, the proposed algorithm is performed with quantization in fig. 2.12. When the number of bit is too small, the impact of message quantization is an obstacle in the convergence of the proposed algorithm. For the convergence of the proposed algorithm, the number of quantization bits per message should be larger than or equal to 12 bits. The number of out-of-sync UEs decreases with larger number of quantization bits in fig. 2.12 although the performance difference is very small. In a quantization of responsibility and availability, 2 byte is enough for each messages as shown in fig. 2.12.

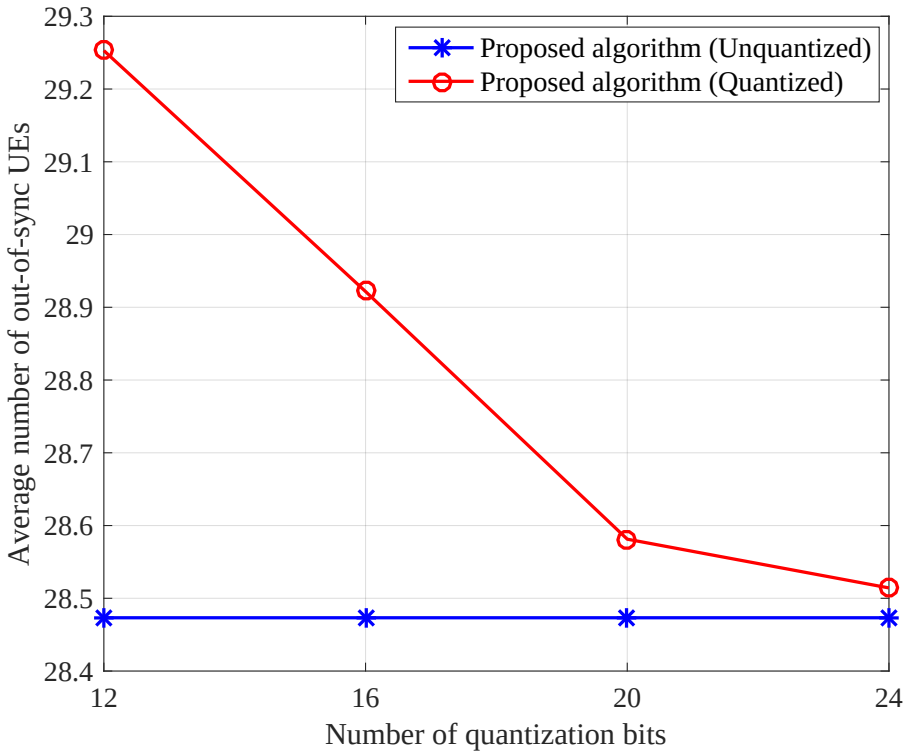

Figure 2.12: Average number of out-of-sync UEs versus the number of quantization bits of messages where $\gamma = -6$ dB, 23 SyncRef UEs, and $N = 500$.

Chapter 3

Reliable Low-Energy Group Formation for Infrastructure-less Public Safety Networks

3.1 System Model and Problem Formulation

3.1.1 Channel Model and Network Structure

An IPSN composed of N UEs is considered. We consider a hierarchical network topology in IPSN composed of GOs and GMs as shown in Fig. 3.1. Black circles, white circles, solid lines, and dashed lines are GOs, GMs, intra-group links between GO and GM, and inter-group links between neighbor GOs, respectively. GOs serve as virtual base stations. GOs coordinate their GMs for synchronizations, resource allocations, and initial attachments. They also relay data to support inter-group communications. Each GM is associated with the nearest GO. A set of GOs is denoted as $\mathcal{V}$, and a set of GMs associated with GO j ($\in \mathcal{V}$) is denoted as $\mathcal{N}_j$.

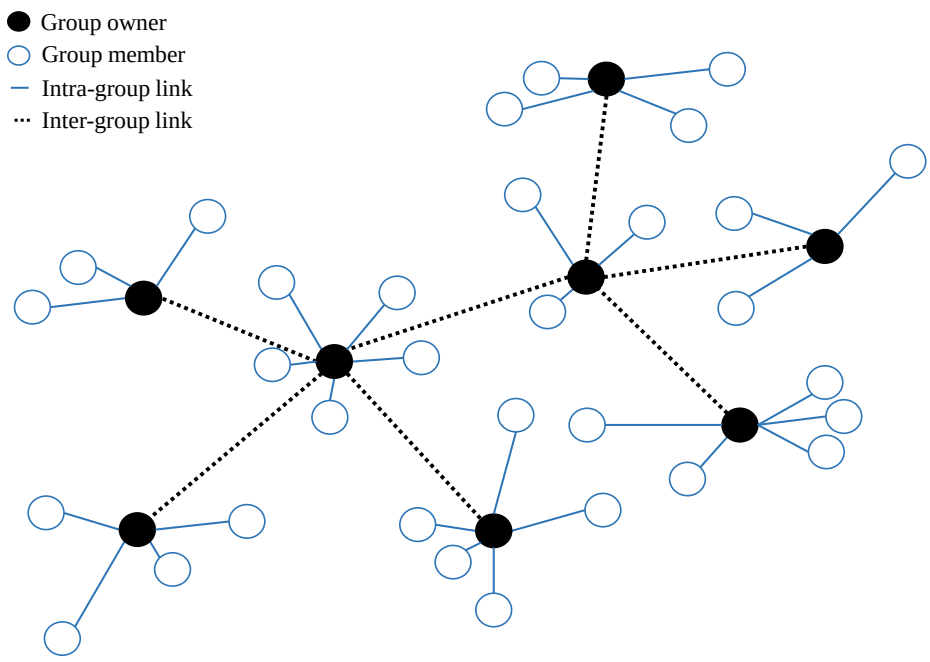

Figure 3.1: Structure of an infrastructure-less public safety network.

We consider path loss channel model defined in 3GPP specification for direct communication between UEs [17, 49]. The received signal power at UE j from UE i is given by

$$P_{ij}^{\text{rx}} = P_i L_0 \left(\frac{d_{ij}}{d_0} \right)^{-\alpha}, \tag{3.1}$$

where P_i, d_{ij}, α, d_0, and L_0 denote the transmit power of UE i, the distance between UE i and UE j, path loss exponent, the reference distance, and the transmission loss at the reference, respectively. Then, the signal-to-noise-ratio (SNR) at UE j from UE i is $\text{SNR}_{ij} = P_{ij}^{\text{rx}}/\sigma^2$, where σ^2 represents the noise power. A link from UE i to UE j is regarded as a reliable link when SNR_{ij} is larger than SNR threshold γ, i.e., $\text{SNR}_{ij} \geq \gamma$. The value of γ depends on modulation, code rate, and acceptable bit error rate. The maximum range of a reliable link with transmit power P and SNR threshold γ can be determined as

$$f(P, \gamma) = d_0 \left(\frac{P L_0}{\gamma \sigma^2} \right)^{1/\alpha}, \text{ for } P \leq \frac{\gamma \sigma^2}{L_0}. \tag{3.2}$$

To organize a reliable clustered hierarchy for an IPSN, two different transmission ranges for reliable links are considered depending on the link types. The transmission range for intra-group links is $r_1 = f(P_1, \gamma_1)$, where P_1 and γ_1 are maximum transmit power for inter-group links, and SNR threshold for intra-group links, respectively. The transmission range for inter-group links is $r_2 = f(P_2, \gamma_2)$, where P_2 and γ_2 are maximum transmit power for inter-group links, and SNR threshold for inter-group links, respectively. Normally, higher transmit power, lower-order modulation, and lower-code rate are required for inter-group links of a wireless backbone, implying that $r_1 \leq r_2$ [19].

3.1.2 Problem Formulation

We focus on minimizing total energy consumption in IPSN. Two types of energy consumption are considered, i.e., the energy consumption for transmissions between GO-GM pairs and the energy consumption for the management of groups. The energy

consumption for the transmissions between GO j and GM i can be expressed using SNR threshold γ_1. The minimum power consumption for transmission between GO j and GM i to be successfully detected at distance d_{ij} is given as

$$w(d_{ij}) = \frac{\gamma_1 \sigma^2}{L_0} \left(\frac{d_{ij}}{d_0} \right)^{\alpha}, \tag{3.3}$$

where σ^2, d_0, and L_0 are noise power, reference distance, and transmission loss at the reference, respectively. The power consumption for the management of each group is a system design parameter related to synchronization, resource allocation, inter-group transmissions, and other system factors. The constant power consumption per cluster is denoted as $\bar{w}_1$ and the power consumption affected by the number of the group members is assumed as $\bar{w}_2$ per intra-cluster link. The power consumption for the management of GO j's cluster can be calculated as $\bar{w}_1 + \sum_{i \in \mathcal{N}_j} \bar{w}_2$. The total power consumption for the management of all clusters in an IPSN can be derived as $\sum_{j \in \mathcal{V}} \bar{w}_1 + \sum_{j \in \mathcal{V}} \sum_{i \in \mathcal{N}_j} \bar{w}_2 = N\bar{w}_2 + \sum_{j \in \mathcal{V}} (\bar{w}_1 - \bar{w}_2)$, where N is the number of UEs in the IPSN. The constant term $N\bar{w}_2$ does not affect the optimization decision of clustering, and $\sum_{j \in \mathcal{V}} (\bar{w}_1 - \bar{w}_2)$ can be converted into $\sum_{j \in \mathcal{V}} \bar{w}$, where $\bar{w} = \bar{w}_1 - \bar{w}_2$. Then, the minimization of the total power is formulated as

$$\text{minimize} \quad \sum_{j \in \mathcal{V}} \sum_{i \in \mathcal{N}_j} w(d_{ij}) + \sum_{j \in \mathcal{V}} \bar{w}. \tag{3.4}$$

In a group-based hierarchy in IPSN, reliable communication between any pair of UEs can be guaranteed by two connectivity conditions, namely, intra-group connectivity and inter-group connectivity. Intra-group connectivity condition implies that each GO should be in the communication range of all GMs associated with it. This condition can be represented as $d_{ij} \leq r_1, \ \forall j \in \mathcal{V}, \ \forall i \in \mathcal{N}_j$. Inter-group connectivity condition implies that any GO should not be isolated from the network of GOs. For the mathematical representation of inter-group connectivity, we define the inter-group adjacency matrix $\mathcal{C}$ and the inter-group connectivity matrix $\mathcal{A}$. Matrix $\mathcal{C}$ is an $L \times L$

matrix whose (l, l') entry is one when the distance between the l-th GO and the l'-th GO is less than r_2, and is zero otherwise, where $L = |\mathcal{V}|$. Matrix $\mathcal{A}$ is an $L \times L$ matrix which is defined as $\mathcal{A} = \sum_{k=1}^{L-1} \mathcal{C}^k$. The (l, l') entry of $\mathcal{C}^k$ is greater than zero if the l-th GO and the l'-th GO are connected via k reliable inter-group links, and is zero otherwise. Thus, $a_{ll'} > 0$ means that the l-th GO and the l'-th GO are connected via one or multiple inter-group reliable links, where $a_{ll'}$ is the (l, l') entry of $\mathcal{A}$. Then, inter-group connectivity condition can be represented as $a_{ll'} > 0,\ \forall\, l, l' \in \{1, 2, ..., L\}$ such that $l \neq l'$.

An optimization problem for energy efficiency and reliability in an IPSN is formulated as

$$\text{minimize} \quad \sum_{j \in \mathcal{V}} \sum_{i \in \mathcal{N}_j} w(d_{ij}) + \sum_{j \in \mathcal{V}} \bar{w} \tag{3.5a}$$

$$\text{subject to} \quad \mathbf{C}_1 : d_{ij} \leq r_1,\ \forall j \in \mathcal{V},\ \forall i \in \mathcal{N}_j, \tag{3.5b}$$

$$\mathbf{C}_2 : a_{ll'} > 0,\ \forall\, l, l' \in \{1, 2, ..., L\} \text{ such that } l \neq l', \tag{3.5c}$$

where (3.5a) represents minimization of total energy consumption through the determination of $\mathcal{V}$, and $\mathcal{N}_j$'s, (3.5b) denotes the connectivity constraints c_1 for intra-group connectivity, and (3.5c) denotes the connectivity constraints c_2 for inter-group connectivity. Note that the clustering problem for minimizing the sum of the energy consumption without any constraints is known to be an NP-hard problem [51]. In addition to this problem, our formulation includes complicated integer constraints to guarantee reliability. This is very challenging, and none of the previous study investigates an efficient solution. To this end, we develop a novel low-complexity algorithm by introducing AP framework.

3.2 Constrained Clustering Algorithm for IPSN

We embed the optimization problem (3.5) into the AP framework through similarity modeling. Then, we develop a low-complexity clustering algorithm for IPSNs.

3.2.1 Similarity Modeling

We embed the optimization problem (3.5) into the AP framework with the following similarity modeling. We define the similarity of UE i to UE j as

$$s(i,j) = \begin{cases} -w(d_{ij}), & \text{if } d_{ij} \leq r_1, \\ -\infty, & \text{otherwise.} \end{cases} \tag{3.6}$$

Then, minimizing total energy consumption in IPSNs is rendered into maximizing the sum of similarities in AP. Our similarity modeling prevents cases in which the distance between a GM and its GO exceeds r_1. In such cases, the sum of the similarities goes to $-\infty$. Therefore, the intra-group connectivity condition is always satisfied. In addition, we define the preference (or self-similarity) of UE j as

$$s(j,j) = \begin{cases} p, & \text{if UE } j \text{ is eligible for a GO,} \\ -\infty, & \text{otherwise,} \end{cases} \tag{3.7}$$

where p takes a value that is less than zero. If UE j is not eligible to become a potential GO due to its high mobility, low residual energy, or UE type, it is precluded by setting $s(j,j)$ to $-\infty$.

3.2.2 Proposed Clustering Algorithm

When a UE detects the disruption of infrastructure, the UE tries to find new clusters of an IPSN to join. If the UE fails to find any available cluster, the UE initiates the procedures to form a clustered hierarchy for an IPSN. To notify the initiation of form-

ing clusters, a flooding-based route discovery can be used, which is well known in distributed network management such as the generation and maintenance of a routing table in ad-hoc network [52, 53, 54]. The flooding-based route discovery is useful in the disruption scenarios because it is assuming ad-hoc network without infrastructure. A UE initiates the procedures to form a clustered hierarchy by broadcasting an information request (IREQ) packet. Some of UEs receiving the IREQ packet become relay nodes and rebroadcast the IREQ packet. The IREQ packet is rebroadcast for a fixed number of hops. The UEs that received IREQ send an information response (IREP) packet to the source UE of the IREQ packet along the reverse path of the IREQ packet. The IREP contains the identification and location information. The source UE performs the proposed clustering algorithm with the collected UE information. If multiple UEs initiate clustering procedures simultaneously, the UE responsible for performing computation can be decided by the pre-determined priority, e.g., the ordering of user identification number. In case of the periodic renewals of clusters, GOs collect UE information of associated GMs and one of GOs collects all the information from GOs to perform the proposed clustering algorithm. After performing the proposed clustering algorithm, the result is delivered to each UE by relaying the result through the selected GOs. According to [52, 53, 54], it is known that the signaling overhead of the flooding-based signaling is manageable if it is performed on a long-term time scale as in the proposed clustering algorithm.

The outputs resulting from AP are a set of GOs, $\mathcal{V}$, and sets of GMs associated with each GO, $\mathcal{N}_j$'s. The intra-group connectivity is always satisfied for all outputs resulting from AP by our similarity modeling. If the inter-group constraint is satisfied, the total power consumption $E(p)$ can be calculated using the power consumption model described in Section 3.2 as

$$E(p) = \begin{cases} \sum_{j\in\mathcal{V}} \sum_{i\in\mathcal{N}_j} w(d_{ij}) + \sum_{j\in\mathcal{V}} \bar{w}, & \text{if } \mathbf{C}_2 \text{ in (5c) is satisfied,} \\ \infty, & \text{otherwise,} \end{cases} \tag{3.8}$$

where $\mathcal{V}$, and $\mathcal{N}_j$ denote the set of GOs, and the sets of GMs associated with GO j, resulting from AP with preference p. If the result of AP does not satisfy the inter-group connectivity constraint, the outputs of AP with p are not valid. In such a case, we consider $E(p)$ as ∞. The proposed clustering algorithm finds the value of p minimizing $E(p)$ as described below. Therefore, the final outputs of the proposed clustering algorithm always satisfy the inter-cluster constraint.

The number of clusters is the key parameter for both total energy consumption and connectivity constraints. As the number of clusters increases, the first term of $E(p)$ decreases and the second term of $E(p)$ increases. If there are too few clusters, the connectivity constraints cannot be satisfied. The proposed clustering algorithm finds the proper number of clusters for the problem (3.5) by controlling the value of p considering total energy consumption and the connectivity constraints. Finding the optimal value of p is a complicated problem, and we propose an efficient method to find the optimal value of p based on what is known as golden section search [55]. Before beginning golden section search, the value of preference changes with the moving rate of ρ to obtain the initial search interval of preference value to find the optimal value of p. The search interval of preference value is represented by the preference triplet $(\phi_{\text{min}}, \phi_{\text{c}}, \phi_{\text{max}})$. The preference triplet $(\phi_{\text{min}}, \phi_{\text{c}}, \phi_{\text{max}})$ consists of the minimum of the search interval ϕ_{min}, the maximum of the search interval ϕ_{max}, and the internal point of the search interval ϕ_{c}. The triplet should satisfy $\phi_{\text{min}} < \phi_{\text{c}} < \phi_{\text{max}}$, $E(\phi_{\text{min}}) > E(\phi_{\text{c}})$, and $E(\phi_{\text{max}}) > E(\phi_{\text{c}})$. After finding the initial preference triplet, the preference triplet is iteratively updated based on golden section search to narrow the search interval of preference value by evaluating the total power consumption at a new value in the search interval, namely ϕ. The overall procedure of the proposed clustering algorithm is shown in Algorithm 2, where $\mathbb{AP}(p)$ represents the optimization via AP with the preference p, and $\mathbb{GSS}(\phi_{\text{min}}, \phi_{\text{c}}, \phi, \phi_{\text{max}})$ denotes the updates of the preference triplet and ϕ based on golden section search.

To find the initial triplet of the preferences, we consider the initial value of p,

Algorithm 2 Proposed clustering algorithm

Initialization: $m = 2$, $p^{(2)} = p^{(1)}\rho$
$E(p^{(1)}) \leftarrow \mathbb{AP}(p^{(1)})$, $E(p^{(2)}) \leftarrow \mathbb{AP}(p^{(2)})$, $\Delta = \text{sign}(E(p^{(1)}) - E(p^{(2)}))$
Phase slowromancapi@. Determination of initial triplet
repeat
    $m = m + 1$
    $p^{(m)} = p^{(1)}\rho^{\Delta(m-1+(\Delta-1)/2)}$
    $E(p^{(m)}) \leftarrow \mathbb{AP}(p^{(m)})$
    $(\phi_{\text{min}}, \phi_{\text{c}}, \phi_{\text{max}}) = (p^{(m-1-\Delta)}, p^{(m-1)}, p^{(m-1+\Delta)})$
until $E(\phi_{\text{min}}) > E(\phi_{\text{c}})$ **and** $E(\phi_{\text{max}}) > E(\phi_{\text{c}})$
Phase slowromancapii@. Golden section search
repeat
    $(\phi_{\text{min}}, \phi_{\text{c}}, \phi, \phi_{\text{max}}) \leftarrow \mathbb{GSS}(\phi_{\text{min}}, \phi_{\text{c}}, \phi, \phi_{\text{max}})$
    $E(\phi) \leftarrow \mathbb{AP}(\phi)$
until $|\phi_{\text{max}} - \phi_{\text{min}}| < \epsilon(|\phi_{\text{c}}| + |\phi|)$
if $E(\phi) > E(\phi_{\text{c}})$ **then** $p_{\text{r}} = \phi_{\text{c}}$
else $p_{\text{r}} = \phi$
end if
return $E(p_{\text{r}}) \leftarrow \mathbb{AP}(p_{\text{r}})$

denoted by $p^{(1)}$, and the moving rate of p, denoted as ρ. Initially, AP is performed with the preference of $p^{(1)}$ and $p^{(2)}$, where $p^{(2)} = p^{(1)}\rho > p^{(1)}$. If $E(p^{(1)}) > E(p^{(2)})$ or $E(p^{(1)}) = E(p^{(2)}) = \infty$, AP is iteratively performed by increasing $p^{(m)} = p^{(1)}\rho^{m-1}$ ($m \geq 3$) until finding M such that $E(p^{(M-1)}) \leq E(p^{(M)})$. The initial triplet of the preferences in this case is $(\phi_{\text{min}}, \phi_{\text{c}}, \phi_{\text{max}}) = (p^{(M-2)}, p^{(M-1)}, p^{(M)})$. If $E(p^{(1)}) < E(p^{(2)})$, AP is iteratively performed by decreasing $p^{(m)} = p^{(1)}\rho^{-(m-2)}$ ($m \geq 3$) until finding M such that $E(p^{(M-1)}) \leq E(p^{(M)})$. The initial triplet of the preferences in this case is $(\phi_{\text{min}}, \phi_{\text{c}}, \phi_{\text{max}}) = (p^{(M)}, p^{(M-1)}, p^{(M-2)})$.

After determining the initial triplet of preferences, the preference value is updated based on golden section search to find the final preference value. Golden section search narrows successively the search interval of preference value by updating the triplet of

preferences. Using $(\phi_{\text{min}}, \phi_{\text{c}}, \phi_{\text{max}})$, a new preference of ϕ is calculated as

$$\phi = \begin{cases} \phi_{\text{c}} + \left(2 - (1+\sqrt{5})/2\right)(\phi_{\text{max}} - \phi_{\text{c}}), & \text{if } \phi_{\text{c}} - \phi_{\text{min}} < \phi_{\text{max}} - \phi_{\text{c}}, \\ \phi_{\text{c}} - \left(2 - (1+\sqrt{5})/2\right)(\phi_{\text{c}} - \phi_{\text{min}}), & \text{otherwise.} \end{cases} \tag{3.9}$$

Among ϕ_{min}, ϕ_{c}, ϕ_{max}, and ϕ, golden section search determines a new triplet of preferences based on the results of AP with the preference of ϕ_{min}, ϕ_{c}, ϕ, and ϕ_{max} as

$$(\phi_{\text{min}}, \phi_{\text{c}}, \phi_{\text{max}}) \leftarrow \begin{cases} (\phi_{\text{min}}, \phi, \phi_{\text{c}}), & \text{if } E(\phi) \leq E(\phi_{\text{c}}) \text{ and } \phi < \phi_{\text{c}}, \\ (\phi, \phi_{\text{c}}, \phi_{\text{max}}), & \text{if } E(\phi) > E(\phi_{\text{c}}) \text{ and } \phi < \phi_{\text{c}}, \\ (\phi_{\text{min}}, \phi_{\text{c}}, \phi), & \text{if } E(\phi) > E(\phi_{\text{c}}) \text{ and } \phi > \phi_{\text{c}}, \\ (\phi_{\text{c}}, \phi, \phi_{\text{max}}), & \text{if } E(\phi) \leq E(\phi_{\text{c}}) \text{ and } \phi > \phi_{\text{c}}. \end{cases} \tag{3.10}$$

The update of the preference triplets terminates if $\phi_{\text{max}} - \phi_{\text{min}} < \epsilon|\phi_{\text{c}} + \phi|$ where ϵ denotes the termination threshold. The final preference value is $p_{\text{r}} = \phi_{\text{c}}$ if $E(\phi) > E(\phi_{\text{c}})$, and the final preference value is $p_{\text{r}} = \phi$ if $E(\phi) < E(\phi_{\text{c}})$. The final clustering outputs are the $\mathcal{V}$ and $\mathcal{N}_j$'s resulting from AP with the preference p_{r}.

3.3 Determination of initial point

The proposed clustering algorithm is based on iterative updates of the AP solution that requires long processing time and high computational complexity. The required number of iterations of the proposed clustering algorithm depends on the choice of the initial value of preference $p^{(1)}$. If the iteration begins with an arbitrary value of $p^{(1)}$, the proposed clustering algorithm finds inefficiently the final value of p. To reduce the number of iterations of the proposed clustering algorithm, we determine the $p^{(1)}$ by estimating the minimum number of clusters, denoted by κ, that satisfies the connectivity constraints.

The estimated minimum number of clusters, κ, depends on r_1, r_2, and S because

the entire area of S should be covered by the clusters, and r_1 and r_2 limit the maximum radii of clusters. When $r_1 < r_2/2$, intra-group connectivity is a major factor that limits the maximum radii of clusters and determines κ. When $r_1 > r_2/2$, inter-group connectivity is a major factor that limits the maximum radii of clusters and determines κ. Therefore, we conclude that κ can be calculated as

$$\kappa = \left\lceil \max\left(\frac{S}{\pi \left(r_1\right)^2}, \frac{S}{\pi \left(r_2/2\right)^2} \right) \right\rceil. \tag{3.11}$$

Then, we determine $p^{(1)}$ which corresponds to κ via their mathematical relation. We determine the relation between the number of clusters and the value of p in AP by averaging the distribution of the UEs.

Lemma 1 *Let N, and S be the number of UEs, and the area, respectively. Then, the relation between the number of clusters, K, and the value of preference p in AP is*

$$p = -\frac{\gamma_1 \sigma^2 (2K + \alpha(N-K))}{K L_0 (\alpha+2)} \left(\frac{S}{\pi K d_0^2} \right)^{\alpha/2}. \tag{3.12}$$

Proof: We define the sum of similarities with the given p and K as

$$R(\mathcal{V}_K, \mathcal{N}_1, ..., \mathcal{N}_K) := \sum_{j \in \mathcal{V}_K} \sum_{i \in \mathcal{N}_j} s(i,j) + \sum_{j \in \mathcal{V}_K} p, \tag{3.13}$$

where $\mathcal{V}_K$ and $\mathcal{N}_j$ denote the set of K GOs and the set of GMs associated with GO j resulting from AP, respectively. The similarity function is assumed as follows:

$$s(i,j) = -w(d_{ij}) = \frac{\gamma_1 \sigma^2}{L_0} \left(\frac{d_{ij}}{d_0} \right)^{\alpha}. \tag{3.14}$$

We assume that GMs are uniformly distributed around the GOs within a circle with a radius of $\sqrt{S/\pi K}$. Then, the expectation of $R(\mathcal{V}_K, \mathcal{N}_1, ..., \mathcal{N}_K)$ is a function of p and

K. It can be derived as

$$\begin{aligned}\bar{R}(p,K) &= \mathbb{E}\Big[R(\mathcal{V}_K,\mathcal{N}_1,...,\mathcal{N}_K)\Big] \\ &= \sum_{j\in\mathcal{V}_K}\sum_{i\in\mathcal{N}_j}\bar{s}(K) + \sum_{j\in\mathcal{V}_K} p \\ &= -\frac{2\gamma_1\sigma^2(N-K)}{L_0(\alpha+2)}\left(\frac{S}{\pi K d_0^2}\right)^{\alpha/2} + Kp.\end{aligned} \tag{3.15}$$

Here, $\bar{s}(K)$ is the mean similarity when K clusters exist; it can be calculated as

$$\bar{s}(K) = \int_0^{2\pi}\int_0^{\sqrt{S/\pi K}} \frac{1}{\pi\left(\sqrt{S/\pi K}\right)^2}\cdot -w(r)\; r\, dr\, d\theta \tag{3.16}$$

$$= -\frac{2\gamma_1\sigma^2}{L_0(\alpha+2)}\left(\frac{S}{\pi K d_0^2}\right)^{\alpha/2}. \tag{3.17}$$

As the number of clusters increases, the sum of similarities decreases while the sum of preferences increases proportionally to the number of clusters. AP autonomously finds the number of clusters that maximizes the sum of similarities with the given value of p as

$$\hat{K} = \arg\max_K \bar{R}(p,K). \tag{3.18}$$

Unfortunately, K is restricted to being an integer. Therefore, $\hat{K}$ can be determined by calculating $\bar{R}(p,K)$ for all K such that $1 \le K \le N$ which is computationally difficult in the case of a large N. Thus, we propose a suboptimal approach with a relaxation technique. That is, K is relaxed as a positive real number of $K \in [1,N]$. This allows us to determine the partial derivative of $\bar{R}(p,K)$ with respect to K as follows:

$$\frac{\partial\bar{R}(p,K)}{\partial K} = \frac{\gamma_1\sigma^2(2K+\alpha(N-K))}{KL_0(\alpha+2)}\left(\frac{S}{\pi K d_0^2}\right)^{\alpha/2} + p. \tag{3.19}$$

For $2 \le \alpha$, $\frac{\partial\bar{R}(p,K)}{\partial K}$ is a continuous and monotonically decreasing function of $K \in [1,N]$ and there exists an unique maximum value of $\bar{R}(p,K)$. The relation between

p and K which makes the result of (3.19) equal to zero is a one-to-one function for $K \in [1, N]$. Therefore, by reformulating $\frac{\partial \bar{R}(p,K)}{\partial K} = 0$ in terms of p, we can ascertain the value of p to create K clusters in AP as

$$p = -\frac{\gamma_1 \sigma^2 (2K + \alpha(N-K))}{K L_0 (\alpha + 2)} \left(\frac{S}{\pi K d_0^2} \right)^{\alpha/2}, \tag{3.20}$$

This completes the proof.

Using Lemma 1, $p^{(1)}$ can be set to

$$p^{(1)} = -\frac{\gamma_1 \sigma^2 (2\kappa + \alpha(N-\kappa))}{\kappa L_0 (\alpha + 2)} \left(\frac{S}{\pi \kappa d_0^2} \right)^{\alpha/2}. \tag{3.21}$$

The derived relation between the number of clusters and the value of p in AP is evaluated in Fig. 3.2 with $N = 400$ and 1000, and the other parameters are same with the parameters described in Table 3.3. Fig. 3.2 shows that the relation is well-estimated such that it can be utilized in the determination of $p^{(1)}$.

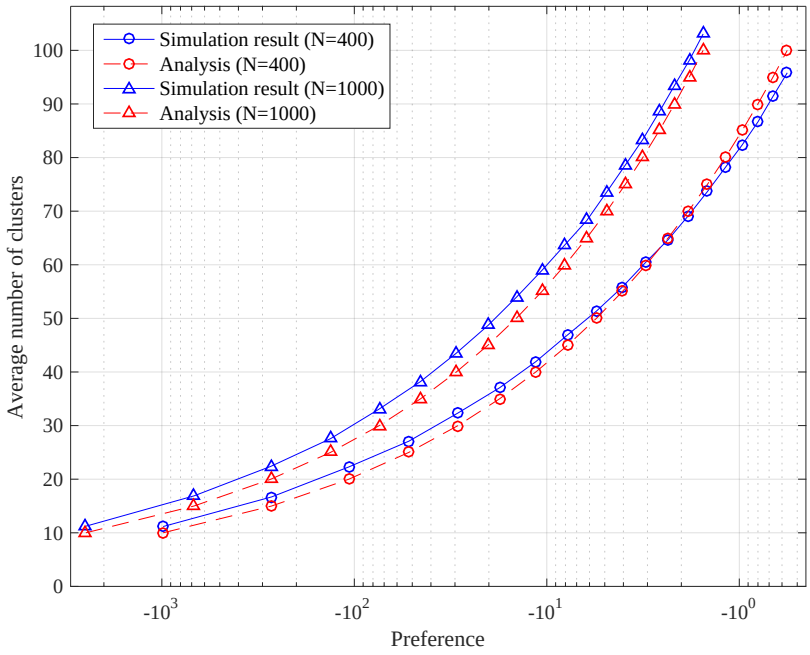

Figure 3.2: Relation between the preference and the average number of clusters.

3.4 Simulation Results

We present the simulation results of the proposed clustering algorithm. A rectangular area of 2 km $\times$ 2 km is considered. A WINNER+ B1 path loss model with $\alpha = 4.37$, $d_0 = 1$ m and $L_0 = 0.068$ is set with a height of 1.5 m and a frequency of 700 MHz, which is the most widely used bandwidth [17, 49]. For intra-group links, SNR threshold γ_1 is set to 9 dB with 16 QAM, a 616/1024 code rate, and 1% bit error rate based on performance evaluation in an LTE system [56]. Similarly, γ_2 is set to 3 dB with QPSK, a 602/1024 code rate, and 1% bit error rate for inter-group links. Maximum transmit powers of $P_1 = 23$ dBm, and $P_2 = 30$ dBm are considered for intra-group link, and inter-group link, respectively. A single set of affinity propagation terminates when the number of iterations is $1,000$ or the decisions of the GOs are identical for 10 iterations. A moving rate of preference is set to $\rho = 0.3$. A termination threshold of $\epsilon = 0.01$ is considered in golden section search. The proposed clustering algorithm is compared with K-means clustering [27], LEACH-C [23], and CDS-based formation [40]. The performances are averaged over 100 independent realizations of user distributions.

Table 3.1: Simulation parameters

Parameter	**Value**
Area, S	2 km $\times$ 2 km
Path loss exponent, α	4.37
Transmission loss at $d_0 = 1$ m, L_0	0.068 dB
Noise power, σ^2	-104 dBm
Maximum Tx power for intra-group link, P_1	23 dBm
Maximum Tx power for inter-group link, P_2	30 dBm
SNR threshold for intra-group link, γ_1	9 dB
SNR threshold for inter-group link, γ_2	3 dB

Fig. 3.3 shows the average number of clusters that minimizes the total energy consumption as a function of $\bar{w}$ for different numbers of UEs, N. The proposed clustering algorithm autonomously finds the number of clusters which minimizes the total energy consumption while satisfying the connectivity constraints. In K-means clustering and

LEACH-C, the average number of clusters that minimizes the total energy consumption is attained by performing the algorithms for $1 \leq K \leq N$ clusters. The value of K that satisfies connectivity constraints in less than 90% of the realizations is excluded from the results for a fair comparison. As the value of $\bar{w}$ increases, the number of clusters decreases in the low $\bar{w}$ region of $\bar{w} \leq 25$ dBm because the total energy consumption can be minimized with less number of clusters. In this region, total energy consumption determines the resulting number of clusters because the connectivity constraints are always satisfied given this number of clusters. On the other hand, the numbers of clusters are nearly identical in the high $\bar{w}$ region of $\bar{w} > 25$ dBm. Despite the fact that fewer clusters is preferred in the perspective of total energy consumption, the number of clusters can not be less than the minimum number of clusters in the region to satisfy connectivity constraints. The proposed clustering algorithm can satisfy the connectivity constraints with fewer clusters because the proposed clustering algorithm is designed considering the connectivity constraint by the similarity modeling. CDS-based formation gives the same results regardless of $\bar{w}$ because CDS-based formation does not consider power consumption. CDS-based formation does not differentiate the maximum ranges according to the link type (intra-group link or inter-group link) [40]. We consider the maximum range for intra-group r_1 as a maximum range in CDS-based formation to guarantee the connectivity constraints satisfied.

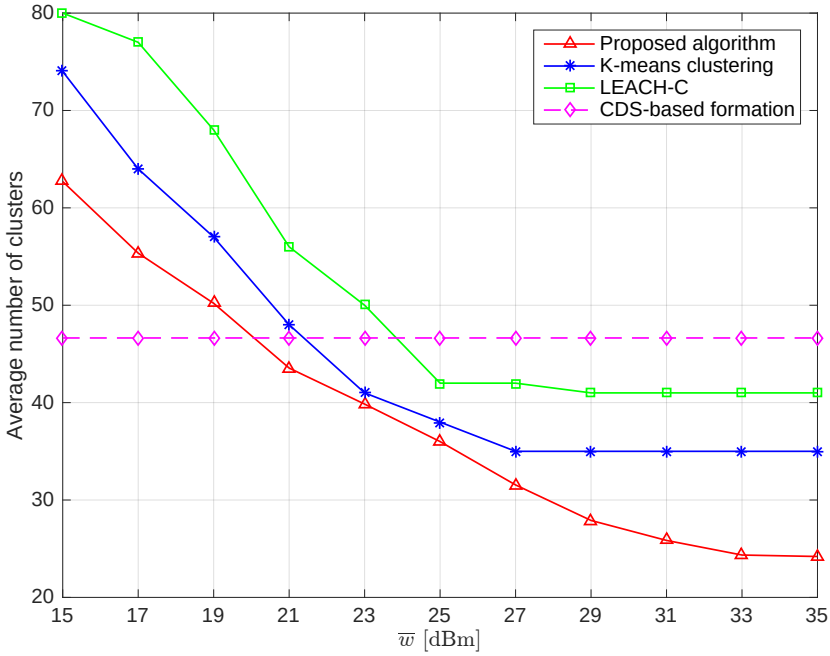

Figure 3.3: Average number of clusters versus the value of $\bar{w}$, where $N = 400$.

Fig. 3.4 shows how the average total energy consumption in the proposed clustering algorithm varies with $\bar{w}$ when the number of UEs is $N = 400$. The proposed clustering algorithm is compared with K-means clustering with $K = 35$, 55, and 74 clusters and LEACH-C with $K = 41$, 61, and 80 clusters. The selected values of K are the value of K minimizing the total power consumption at $\bar{w} = 35$ dBm in Fig 3.3, the value of K minimizing the total power consumption at $\bar{w} = 15$ dBm in Fig 3.3, and the mean of these two values. CDS-based formation creates the same number of clusters regardless of $\bar{w}$ as shown in in Fig 3.3. The proposed clustering algorithm shows the lowest energy consumption compared to K-means clustering, LEACH-C, and CDS-based formation, irrespective of the value of $\bar{w}$. Specifically, the proposed clustering algorithm provides less energy consumption than K-means clustering, LEACH-C, and CDS-based formation by up to 31% in the high $\bar{w}$ region of $\bar{w} > 25$ dBm where connectivity constraints dominate the resulting number of clusters. The performance gain of the proposed clustering algorithm in the high $\bar{w}$ region comes from the relatively small number of clusters satisfying the connectivity constraints in the proposed clustering algorithm. In the region of $\bar{w} < 25$ dBm, the proposed clustering algorithm provides better power minimization than K-means clustering by about 12%. The performance gain of the proposed clustering algorithm in the low $\bar{w}$ region comes from the outstanding clustering performance of the AP framework.

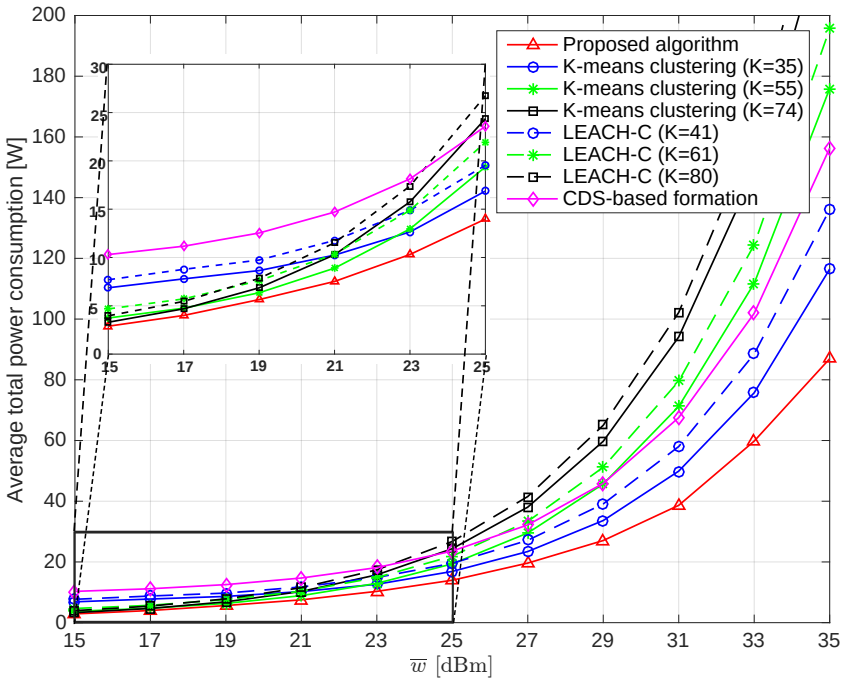

Figure 3.4: Average total power consumption versus the value of $\bar{w}$, where $N = 400$.

Fig. 3.5 compares the average total energy consumption in the proposed clustering algorithm with those of K-means clustering and LEACH-C as a function of the number of UEs when $\bar{w} = 30$ dBm. The selected values of $K = 35$ for K-means and $K = 41$ for LEACH-C are the minimum number of clusters satisfying the connectivity constraints in more than 90% of the realizations because $\bar{w} = 30$ dBm is in the high $\bar{w}$ region. The average total energy consumption gradually increases with the number of UEs. The proposed clustering algorithm shows more energy saving than the existing clustering algorithms by 26% when $N = 200$ and by 12% when $N = 600$. As noted above, the performance gain of the proposed clustering algorithm comes from the relatively small number of clusters in the high $\bar{w}$ region. As the number of UEs increases, the performance difference decreases because the portion of $\sum_{j \in \mathcal{V}} \bar{w}$ out of the total power consumption decreases.

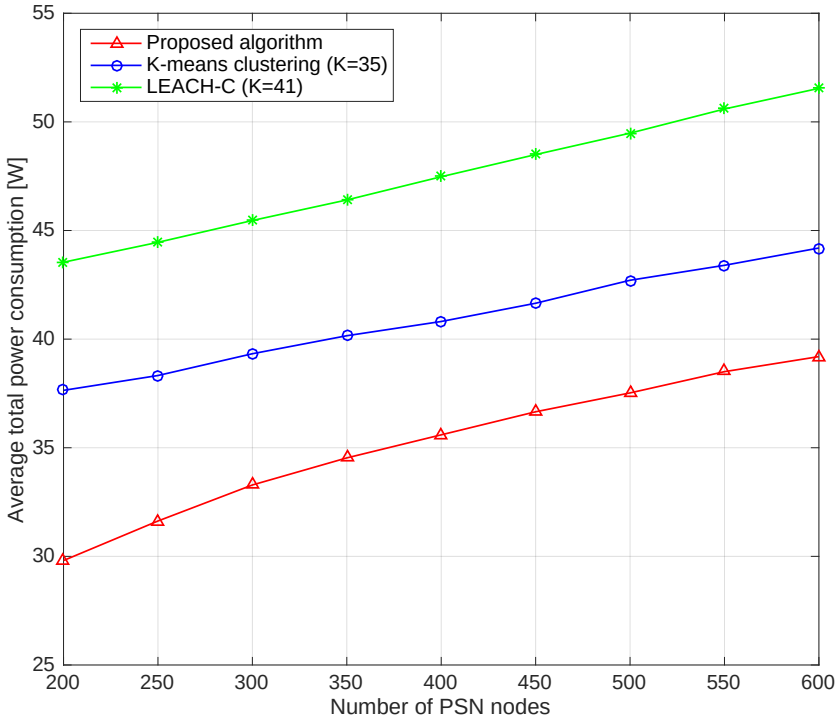

Figure 3.5: Average total power consumption versus the number of UEs, where $\bar{w} = 30$ dBm.

Similarly, Fig. 3.6 compares the average total energy consumption in the proposed clustering algorithm with that of K-means clustering and LEACH-C as a function of the number of UEs when $\bar{w} = 20$ dBm in the low $\bar{w}$ region. $K = 41$, 53, and 65 are selected for K-means clustering and $K = 45$, 65, and 84 are selected for LEACH-C. The selected values of K are the value of K minimizing the total power consumption at $N = 200$, the value of K minimizing the total power consumption at $N = 800$, and the mean of these two values. As the number of UEs in IPSN increases, more number of clusters are created to minimize the total power consumption. The proposed clustering algorithm reduces the total power consumption by about 12% compared to K-means clustering and by about 30% compared to LEACH-C. The performance gain which comes from the outstanding clustering performance of the AP framework remains steady regardless of the number of UEs.

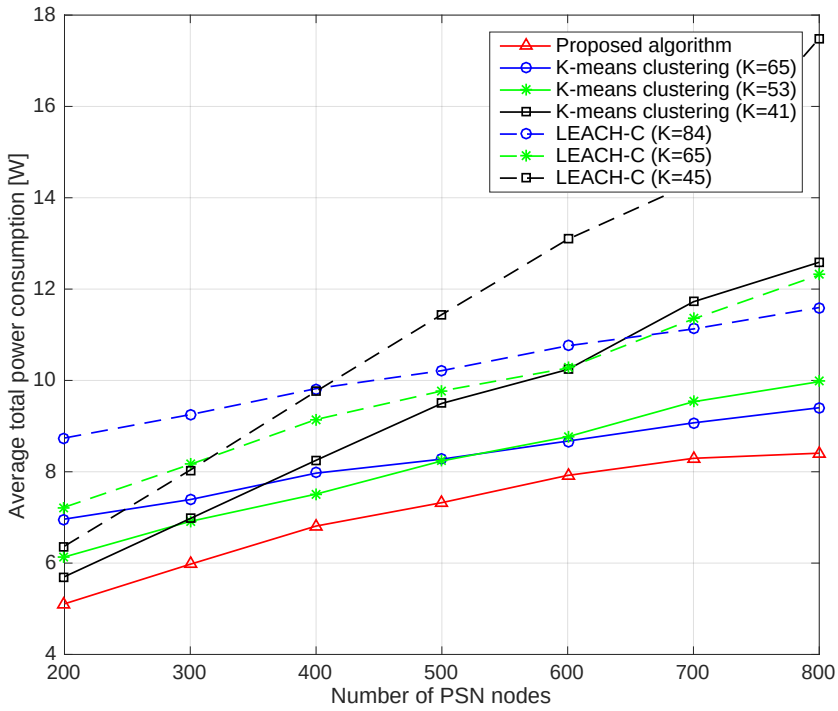

Figure 3.6: Average total power consumption versus the number of UEs, where $\bar{w} = 20$ dBm.

Table 3.2 shows how the average total power consumption varies with the number of iterations, denoted by $t_{\max}$, in the proposed clustering algorithm. Case A considers $N = 400$, and $\bar{w} = 20$ dB, Case B considers $N = 400$, and $\bar{w} = 30$ dB, and Case C considers $N = 800$, and $\bar{w} = 20$ dB. In general, larger number of iterations improves the performance of the proposed algorithm. However, the algorithm complexity can be considerably reduced by sacrificing the performance slightly. Note that the proposed clustering algorithm with $t_{\max} = 70$ still notably outperforms the conventional clustering algorithm. Considering that the proposed clustering algorithm is performed on a long-term time scale as described in Fig. 3.9, the computation cost for the proposed clustering algorithm is manageable.

Table 3.2: Average total power consumption vs number of iterations

	Proposed algorithm [W]				K-means
# of iterations	100	90	80	70	clustering [W]
Case A	6.8	6.8	6.9	7.1	7.5
Case B	35.5	36.2	37.7	38.5	41.1
Case C	8.3	8.4	8.5	8.7	9.3

Fig. 3.7 shows the empirical cumulative distribution function (CDF) of the number of hops between UEs, where $N = 400$. The average latency in packet delivery between the UEs is proportional to the number of hops between them. More than 90% UE pairs can deliver packets to each other within 4 hops when the simulation area is 2 km $\times$ 2 km. The structures of clustered hierarchies are different at $\bar{w} = 20$ dB and 30 dB due to the different number of clusters. However, the average number of hops between any two pairs is similar.

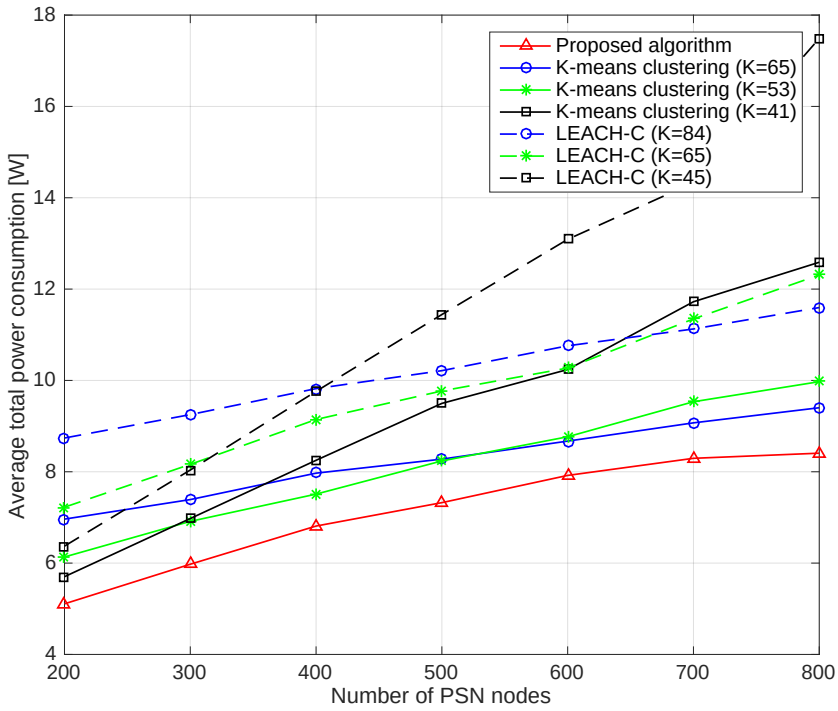

Figure 3.7: Empirical CDF of the number of hops, where $N = 400$.

To provide the simulation results in more practical scenarios, Option 1, which defines the layout for the simulation of IPSNs in 3GPP LTE [17], is used in Fig. 3.8 and Fig. 3.9. The parameters defined in Option 1 are described in Table 4. eNodeBs are used only for describing the UE distributions and it is assumed that no eNodeB is enabled for IPSNs as defined in [17]. Shadowing is assumed to follow log-normal distribution and the shadowing standard deviation, denoted by σ_{sh}, is varied from $\sigma_{\text{sh}} = 0$ to 10 dB. In the practical model, the connectivity constraints cannot be always guaranteed in the proposed clustering algorithm due to the channel fluctuation. We define the outage probability as the probability that the received SNR at a UE from its GO is less than the required threshold γ_1. The outage probability shows how reliable the links between GMs and GOs are in a fading model and a mobility model.

Table 3.3: Simulation parameters for more practical scenarios

Parameter2	**Value**
ISD	500 m
Number of eNodeB	19
Number of sector per eNodeB	3
Number of UE per sector	10 (Uniform, Outdoor)
eNodeBs enabled	0%
Shadowing	i.i.d.

Fig. 3.8 shows the average outage probability in the proposed clustering algorithm as a function of the shadowing standard deviation. The proposed clustering algorithm always satisfies the connectivity constraints and the outage probability equals zero when shadow fading is not considered. As the shadowing standard deviation increases, the outage probability increases. The proposed clustering algorithm can reduce the outage probability by conservative setting in the connectivity constraints. In other words, the outage probability can be reduced if r_1 and r_2 are set to smaller values. The conservative setting for reliability results in higher power consumption in the proposed clustering algorithm. The tradeoff between the reliability and the power consumption

should be considered in the practical implementations.

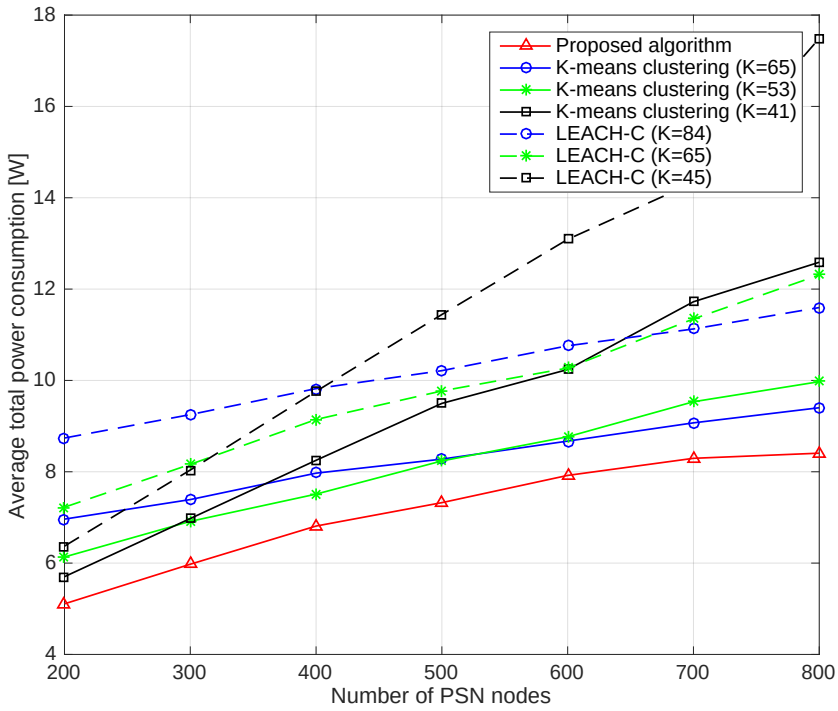

Figure 3.8: Average outage probability versus the shadowing standard deviation.

Fig. 3.9 shows the average outage probability in the proposed clustering algorithm as a function of time and UE speed, denoted by v. A random walk mobility model [57], which is one of the most employed models used for ad hoc network [58] and sensor network [59], is used in the mobility pattern of UEs. To focus on the impact of mobility in the proposed clustering algorithm, the impact of shadow fading is excluded here. With no mobility of UEs, the outage probability equals zero by the clustering result ensuring the connectivity constraints from the clustering algorithm. As UEs move faster, the outage probability increases fast and the renewal of clusters should be performed more frequently to maintain a reliable hierarchy. However, the renewal of clusters every 10 minutes is enough to maintain a reliable hierarchy even when $v = 9$ km/h. The outage probability can be reduced by setting r_1 and r_2 to smaller values and the similar tradeoff between the reliability and the power consumption with the fading model exists in the mobility model.

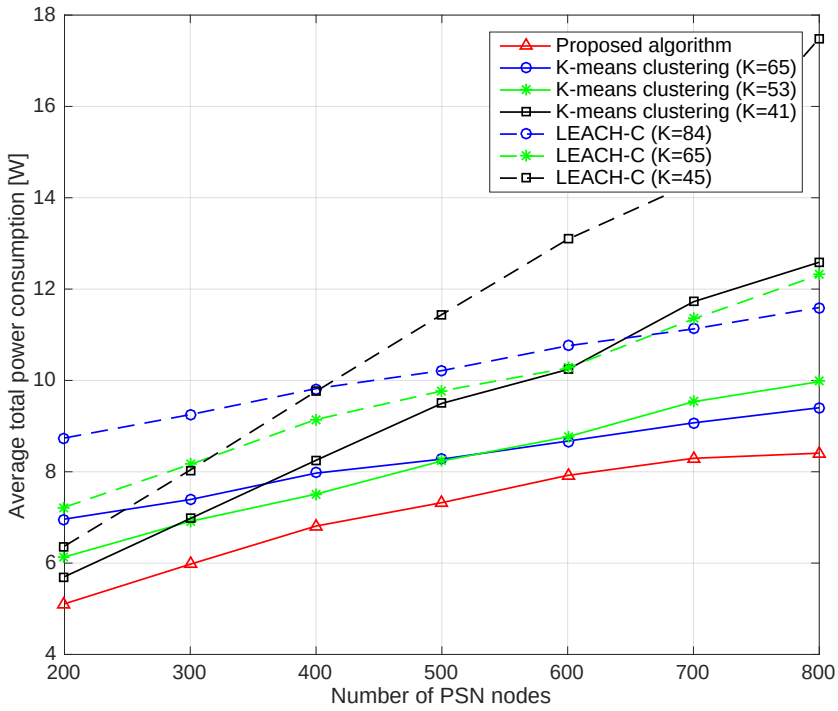

Figure 3.9: Average outage probability versus time, where $\bar{w} = 25$ dBm.

Chapter 4

Conclusion and Future Work

4.1 Conclusion

In the first part of the dissertation in Chapter 2, a distributed synchronization algorithm in the affinity propagation framework is developed. By allowing local message-passing, the proposed algorithm enables autonomous decisions to determine SyncRefs and SyncGroups. Simulation results shows that the proposed algorithm considerably outperforms the existing scan-and-select strategy.

In Chapter 3, a novel clustering algorithm based on affinity propagation is proposed to provision both energy efficiency and reliability in IPSNs. As a key novelty, we embed the optimization problem of IPSNs into the AP framework by means of similarity modeling, and proposing an efficient method to find the number of GOs based on golden section search. The proposed clustering algorithm adaptively determines the number of clusters that minimizes total energy consumption while satisfying the connectivity constraints. The simulation results have shown that the proposed clustering algorithm considerably outperforms K-means clustering, LEACH-C, and CDS-based formation in various environments.

4.2 Future Work

Our future research will include an extension of the proposed algorithm to multi-hop synchronization model. Also, future research directions include studies of the impact of UE mobility, heterogeneous traffic patterns, and different types of device type. The consideration of more practical scenarios will facilitate the implementation of the proposed algorithms. The joint optimization of SyncRef selection and group formation will be investigated to enhance the overall performance compared to ISPN formation by the respective optimization of SyncRef selection and group formation.

Bibliography

[1] T. Doumi, M. Dolan, S. Tatesh, A. Casati, G. Tsirtsis, K. Anchan, and D. Flore, "LTE for public safety networks," *IEEE Communications Magazine*, vol. 51, no. 2, pp. 106-112, Feb. 2013.

[2] Technical Advisory Board for First Responder Interoperability, "Recommended minimum technical requirements to ensure nationwide interoperability for the nationwide public safety broadband network," Tech. Rep., May 2012.

[3] D. Buchanan, "700 MHz public safety broadband task force report and recommendations," NPSTC, Sept. 2009.

[4] R. Rouil, A. Izquierdo, C. Gentile, D. Griffith, and N. Golmie, Nationwide Public Safety Broadband Network Deployment: Network Parameter Sensitivity Analysis, 2015.

[5] R. Ferrus, O. Sallent, G. Baldini, and L. Goratti, "LTE: the technology driver for future public safety communications," *IEEE Communications Magazine*, vol. 51, no. 10, pp. 154-161, October 2013.

[6] "Requirements for support of radio resource management," The 3rd Generation Partnership Project (3GPP), TS 36.133 V13.0.0, July 2015.

[7] G. Baldini, S. Karanasios, D. Allen, and F. Vergari, "Survey of wireless communication technologies for public safety," *IEEE Communications Surveys Tutorials*, vol. 16, no. 2, pp. 619-641, Second Quarter 2014.

[8] "Radio Resource Control (RRC); Protocol specification," The 3rd Generation Partnership Project (3GPP), TS 36.331 V12.5.0, Mar. 2015.

[9] B. J. Frey and D. Dueck, "Clustering by passing messages between data points," *Science*, vol. 315, no. 5814, pp. 972-976, 2007.

[10] M. Shamaiah, S. H. Lee, S. Vishwanath, and H. Vikalo, "Distributed algorithms for spectrum access in cognitive radio relay networks," *IEEE Journal on Selected Areas in Communications*, vol. 30, no. 10, pp. 1947-1957, Nov. 2012.

[11] S. H. Lee and I. Sohn, "Distributed relay pairing for bandwidth exchange based cooperative forwarding," *IEEE Communications Letters*, vol. 19, no. 3, pp. 459-462, Mar. 2015.

[12] S. H. Lee and I. Sohn, "Affinity propagation for energy-effcient BS operations in green cellular networks," *IEEE Transactions on Wireless Communications*, vol. 14, no. 8, pp. 4534-4545, Aug. 2015.

[13] C. Shea, B. Hassanabadi, and S. Valaee, "Mobility-based clustering in VANETs using affinity propagation," in *IEEE Global Telecommunications Conference*, Nov 2009, pp. 1-6.

[14] ETSI, "Terrestrial Trunked Radio (TETRA); Voice plus Data (V+D); Designer's Guide; Part 3: Direct Mode Operation (DMO)," European Telecommunications Standards Institute (ETSI), TR 300-3 V1.3.3, June 2009.

[15] "Service requirements for the Evolved Packet System (EPS)," The 3rd Generation Partnership Project (3GPP), TS 22.278 V13.2.0, Dec. 2014.

[16] "Feasibility study for proximity services," The 3rd Generation Partnership Project (3GPP), TR 22.803 V12.2.0, June 2013.

[17] "Study on LTE Device-to-Device proximity services," The 3rd Generation Partnership Project (3GPP), TR 36.843 V12.0.1, Mar. 2014.

[18] "Study on architecture enhancements to support Proximity-based Services (ProSe)," The 3rd Generation Partnership Project (3GPP), TR 23.703 V12.0.0, Feb. 2014.

[19] X. Liu, "A survey on clustering routing protocols in wireless sensor networks," *Sensors*, vol. 12, no. 8, pp. 11113-11 153, 2012.

[20] A. A. Abbasi and M. Younis, "A survey on clustering algorithms for wireless sensor networks," *Computer Communications*, vol. 30, no. 14, pp. 2826-2841, 2007.

[21] A. Anand and N. Mehta, "Quick, decentralized, energy-efficient one-shot max function computation using timer-based selection," *IEEE Transactions on Communications*, vol. 63, no. 3, pp. 927-937, Mar. 2015.

[22] W. Heinzelman, A. Chandrakasan, and H. Balakrishnan, "An application-specific protocol architecture for wireless microsensor networks," *IEEE Transactions on Wireless Communications*, vol. 1, no. 4, pp. 660-670, Oct. 2002.

[23] M. Tripathi, M. Gaur, V. Laxmi, and R. Battula, "Energy efficient LEACH-C protocol for wireless sensor network," in *Proceedings of International Conference on Computational Intelligence and Information Technology*, Oct. 2013, pp. 402-405.

[24] F. Zhao, Y. Xu, and R. Li, "Improved LEACH routing communication protocol for a wireless sensor network," *International Journal of Distributed Sensor Networks*, vol. 2012, pp. 1-6, 2012.

[25] T. Voigt, A. Dunkels, J. Alonso, H. Ritter, and J. Schiller, "Solar-aware clustering in wireless sensor networks," in *Proceedings of International Symposium on Computers and Communications*, vol. 1, June 2004, pp. 238-243.

[26] T. Murata and H. Ishibuchi, "Performance evaluation of genetic algorithms for flowshop scheduling problems," in *Proceedings of IEEE Conference on Evolutionary Computation*, June 1994, pp. 812-817 vol.2.

[27] D. Mechta, S. Harous, I. Alem, and D. Khebbab, "LEACH-CKM: Low energy adaptive clustering hierarchy protocol with K-means and MTE," in *Proceedings of International Conference on Innovations in Information Technology*, Nov. 2014, pp. 99-103.

[28] G. Y. Park, H. Kim, H. W. Jeong, and H. Y. Youn, "A novel cluster head selection method based on K-means algorithm for energy efficient wireless sensor network," in *Proceedings of International Conference on Advanced Information Networking and Applications Workshops*, Mar. 2013, pp. 910-915.

[29] P. Sasikumar and S. Khara, "K-means clustering in wireless sensor networks," in *Proceedings of International Conference on Computational Intelligence and Communication Networks*, Nov. 2012, pp. 140-144.

[30] J. Macqueen, "Some methods for classification and analysis of multivariate observations," in *Proceedings of Berkeley Symposium on Mathematical Statistics and Probability*, 1967, pp. 281-297.

[31] S. Tyagi, S. Tanwar, S. K. Gupta, N. Kumar, S. Misra, J. P. C. Rodrigues, and S. Ullah, "Bayesian coalition game-based optimized clustering in wireless sensor networks," in *Proceedings of IEEE International Conference on Communications (ICC)*, June 2015, pp. 3540-3545.

[32] D. Wu, Y. Cai, L. Zhou, and J. Wang, "A cooperative communication scheme based on coalition formation game in clustered wireless sensor networks," *IEEE Transactions on Wireless Communications*, vol. 11, no. 3, pp. 1190-1200, March 2012.

[33] W. Saad, Q. Zhu, T. Basar, Z. Han, and A. Hjorungnes, "Hierarchical network formation games in the uplink of multi-hop wireless networks," in *Proceedings of IEEE Global Telecommunications Conference*, Nov 2009, pp. 1-6.

[34] W. Saad, Z. Han, M. Debbah, A. Hjorungnes, and T. Basar, "Coalitional game theory for communication networks," *IEEE Signal Processing Magazine*, vol. 26, no. 5, pp. 77-97, September 2009.

[35] X. Lu, P. Wang, and D. Niyato, "Hierarchical cooperation for operator-controlled device-to-device communications: A layered coalitional game approach," in *Proceedings of IEEE Wireless Communications and Networking Conference (WCNC)*, March 2015, pp. 2056-2061.

[36] Y. Xiao, K. C. Chen, C. Yuen, Z. Han, and L. A. DaSilva, "A bayesian overlapping coalition formation game for device-to-device spectrum sharing in cellular networks," *IEEE Transactions on Wireless Communications*, vol. 14, no. 7, pp. 4034-4051, July 2015.

[37] J. Yu, N. Wang, G. Wang, and D. Yu, "Connected dominating sets in wireless ad hoc and sensor networks – a comprehensive survey," *Computer Communications*, vol. 36, no. 2, pp. 121-134, 2013.

[38] K. M. Alzoubi, P.-J. Wan, and O. Frieder, "Distributed heuristics for connected dominating sets in wireless ad-hoc networks," *Journal of Communications and Networks*, vol. 4, no. 1, pp. 22-29, 2002.

[39] J. Blum, M. Ding, A. Thaeler, and X. Cheng, "Connected Dominating Set in Sensor Networks and MANETs," *Handbook of Combinatorial Optimization: Supplement Volume B*, pp. 329-369, 2005.

[40] D. Kim, Y. Wu, Y. Li, F. Zou, and D.-Z. Du, "Constructing minimum connected dominating sets with bounded diameters in wireless networks," *IEEE Transactions on Parallel and Distributed Systems*, vol. 20, no. 2, pp. 147-157, Feb. 2009.

[41] S. Guha and S. Khuller, "Approximation algorithms for connected dominating sets," *Algorithmica*, vol. 20, no. 4, pp. 374-387, 1998.

[42] L. Ruan, H. Du, X. Jia, W. Wu, Y. Li, and K.-I. Ko, "A greedy approximation for minimum connected dominating sets," *Theoretical Computer Science*, vol. 329, no. 1, pp. 325-330, 2004.

[43] I. Sohn, S. H. Lee, and J. Andrews, "Belief propagation for distributed downlink beamforming in cooperative MIMO cellular networks," *IEEE Transactions on Wireless Communications*, vol. 10, no. 12, pp. 4140-4149, Dec. 2011.

[44] "Physical Channels and Modulation," The 3rd Generation Partnership Project (3GPP), TS 36.211 V12.7.0, Sept. 2015.

[45] W. C. Jakes and D. C. Cox, *Microwave Mobile Communications*. Wiley-IEEE Press, 1994.

[46] I. E. Givoni and B. J. Frey, "A binary variable model for affnity propagation," *Neural computation*, vol. 21, no. 6, pp. 1589-1600, 2009.

[47] F. R. Kschischang, B. J. Frey, and H. A. Loeliger, "Factor graphs and the sum-product algorithm," *IEEE Transactions on Information Theory*, vol. 47, no. 2, pp. 498-519, Feb 2001.

[48] M. Wang, W. Zhang, W. Ding, D. Dai, H. Zhang, H. Xie, L. Chen, Y. Guo, and J. Xie, "Parallel clustering algorithm for large-scale biological data sets," PloS one, vol. 9, no. 4, p. e91315, 2014.

[49] J. Meinila, P. Kyosti, L. Hentila, T. Jamsa, E. Suikkanen, E. Kunnari, and M. Narandzic, "D5.3: WINNER+ final channel models," Wireless World Initiative New Radio WINNER, 2010.

[50] "Details of synchronization procedure," Qualcomm Incorporated, 3GPP Tdoc R1-145063, 3GPP TSG-RAN WG1 #79, Nov. 2014.

[51] O. Kariv and S. L. Hakimi, “An algorithmic approach to network location problems II: The p-medians,” *SIAM Journal on Applied Mathematics*, vol. 37, no. 3, pp. 539-560, 1979.

[52] C. E. Perkins and E. M. Royer, “Ad-hoc on-demand distance vector routing,” in *Proceedings of IEEE Workshop on Mobile Computing Systems and Applications*, Feb 1999, pp. 90-100.

[53] H. Dubois-Ferriere, M. Grossglauser, and M. Vetterli, “Age matters: efficient route discovery in mobile ad hoc networks using encounter ages,” in *Proceedings of the 4th ACM international symposium on Mobile ad hoc networking & computing*. ACM, 2003, pp. 257-266.

[54] X. M. Zhang, E. B. Wang, J. J. Xia, and D. K. Sung, “A neighbor coverage-based probabilistic rebroadcast for reducing routing overhead in mobile ad hoc networks,” *IEEE Transactions on Mobile Computing*, vol. 12, no. 3, pp. 424-433, March 2013.

[55] J. Kiefer, “Sequential minimax search for a maximum,” *Proceedings of the American Mathematical Society*, vol. 4, no. 3, pp. 502-506, 1953.

[56] J. Blumenstein, J. Ikuno, J. Prokopec, and M. Rupp, “Simulating the long-term evolution uplink physical layer,” in *Proceedings of ELMAR*, Sept. 2011, pp. 141-144.

[57] T. Camp, J. Boleng, and V. Davies, “A survey of mobility models for ad hoc network research,” *Wireless communications and mobile computing*, vol. 2, no. 5, pp. 483-502, 2002.

[58] J. Liu, H. Nishiyama, N. Kato, T. Kumagai, and A. Takahara, “Toward modeling ad hoc networks: current situation and future direction,” *IEEE Wireless Communications*, vol. 20, no. 6, pp. 51-58, 2013.

[59] R. Bellazreg and N. Boudriga, “Dyntunkey: a dynamic distributed group key tunneling management protocol for heterogeneous wireless sensor networks,” *EURASIP Journal on Wireless Communications and Networking*, vol. 2014, no. 1, pp. 1-19, 2014.

초 록

재난 통신망은 생명 및 재산을 구하기 위한 특수한 목적을 가진 무선 통신망을 말한다. 재난 통신망은 상업적 목적의 무선 통신망과는 분리되어 발전되어 왔는데, 이는 재난 통신망이 상업 통신망과는 다른 요구조건과 규제요건을 만족시켜야 하기 때문이다. 멀티미디어 데이터의 전송에 대한 요구가 늘어나면서 현재의 음성 전송 위주의 재난 통신망 기술은 높은 전송량과 다양한 종류의 서비스를 제공해야 하는 어려움에 직면하였다. 재난 통신망은 셀룰러 기지국이 존재하지 않거나 붕괴된 상황에서도 경고 문자, 사진, 영상 등의 긴급 재난 정보를 안정적으로 전송 가능해야 한다. 이와 같은 재난 통신망의 요구조건을 만족하는 기술개발을 위해 ABSOLUTE (Aerial Base Station with Opportunistic Links for Unexpected & TEmporary events), Alert4All (Alert for All), MAIA (Mobile Alert InformAtion system using satellites) 등의 다양한 연구 프로젝트가 출범되었다. 이러한 연구 프로젝트들은 위성 통신, 벌룬을 이용한 공중 기지국 기반의 통신, 단말 간의 직접 통신을 이용하여 기지국이 없는 환경에서의 재난 통신을 지원하는 기술을 연구하였다. 본 학위 논문에서는 인프라가 없는 환경에서 단말 간 직접 통신에 대한 연구를 수행한다. LTE, TETRA, TETRAPOL, DMR 등의 표준에서 인프라가 없는 환경에서의 단말 간 직접 통신을 지원한다. 단말 간 직접 통신은 인공위성이나 공중 기지국과의 통신이 불가능한 저기능 단말에서도 지원가능하다는 장점이 있다. 본 학위 논문의 Chapter 1에서는 인프라가 없는 재난 통신망에서의 분산적 동기화 기법을 제안하였다. 제안된 알고리즘은 효율적으로 동기화 그룹과 동기기준단말을 선택하여 out-of-sync 단말의 수를 최소화하는 것을 목표로 한다. 이를 위하여 각 단말의 분산적인 동작으로 알고리즘

을 설계할 수 있는 affinity propagation 기법을 도입하였다. Affinity propagation이란 기계학습 분야에서 제안된 메시지 전달 기법을 기반으로 한 최신의 클러스터링 기술이다. 이를 통해 제안된 알고리즘은 인프라가 없는 재난 통신망에서 각 단말은 협력적으로 메시지를 주고 받으며 동기화 그룹과 동기기준단말을 선택한다. 시뮬레이션을 통한 수치결과를 살펴본 결과, 제안된 알고리즘은 기존의 동기화 방식인 scan-and-select 기법보다 40%까지 out-of-sync 단말을 줄일 수 있음을 확인하였다. 본 학위 논문의 Chapter 2에서는 인프라가 없는 재난 통신망에서의 정보 전달에 있어 에너지 효율성과 안정성을 고려한 그룹 형성 기법에 대한 연구를 수행하였다. 인프라가 없는 환경에서 일부의 단말은 가상의 기지국의 역할을 수행하는 그룹주관단말이 되고 나머지 단말들은 그룹주관단말에 속하는 그룹소속단말이 된다. 그룹화 방식에 따라 재난통신망 전체에서 소모되는 에너지와 전송 안정성이 정해지는데 이러한 그룹화 문제를 클러스터링 문제로 정리하였다. 본 학위논문에서는 affinity propagation 기법을 기반으로 전송 안정성을 보장하면서도 에너지 소모를 최소화하기 위한 알고리즘을 제안하였다. 시뮬레이션을 통한 수치결과를 살펴본 결과 안정성을 보장하면서도 기존의 클러스터링 알고리즘과 비교했을 때 최대 31%까지 에너지 소모를 줄일 수 있음을 확인하였다.

주요어: 인프라가 없는 환경, 재난 통신망, 동기화, 그룹 형성 기법, 친밀도 전파
학번: 2008-22936